# SHALE SWELLING AND STABILITY, MODEL AND SIMULATION, GULF OF MEXICO

**Liberto de Pablo[1], María de L. Chávez[2], Cristina Avilés[3], Carlos Islas[4]**
**[1]Instituto de Geología, Universidad Nacional A. de México; [2]Facultad de Química, Universidad Nacional A. de México; [3]Instituto Mexicano del Petróleo; [4]Exploración-Producción, Petróleos Mexicanos (PEMEX)**

## ABSTRACT

Swelling and overpressuring in shales in oil reservoirs are associated, among others, with theclay minerals in the shale, their evolution through burial diagenesis and reaction with brines, pore fluids, and drilling muds. The shale studied is from the Southern Gulf of Mexico, 2465 m deep, Oligocene, containing 50.8% clay minerals (random and ordered illite(0.5)-smectite, illite(0.75)-smectite, random chlorite(0.9)-smectite, smectite dioctahedral, chlorite, illitic material, and odinite), having a CEC of 83.12 meq/100 g. Leached in water at 22°C and at the burial temperature of 80°C, releases $Na^+$ and $Mg^{2+}$ and changes the mineralogy to predominant Fe-chlorite, odinite, and illitic material. Rehydrated shale, reacting at 22°C with $Na^+$, $K^+$, $Ca^{2+}$, or $Mg^{2+}$ solutions, looses $Na^+$ to form two-water layer smectite when $Na^+$ is the reacting electrolyte, or adsorbs $K^+$, $Ca^{2+}$, or $Mg^{2+}$ from the solutions to form random illite-smectite and chlorite-smectite interstratifications. At the burial temperature of 80°C, weak electrolytes partially transform illite-smectite and chlorite-smectite to illitic material and odinite (or possibly Fe-rich chlorite). Upon increasingly longer reaction times, illitic material and odinite are replaced by ordered illite-smectite, chlorite-smectite and smectite. Strong electrolytes, at 80°C, form ordered illite-smectite when Na or K are the electrolytes; random and ordered illite-smectite and chlorite-smectite interstratifications when is Ca, and random illite-smectite and chlorite-smectite when is Mg. Washing with $H_2O$ the cation saturated clays develops odinite and illitic material. Clays assemblages at ambient 22°C are different from those stable at the burial temperature of 80°C. The transformations imply changes in the (00l) spacings, in the clay surface, and in the surrounding fluid that lead to instability on the shale. The changes are interpreted in terms of the double-layer theory and associated with a mechanical model to design drilling muds that would maintain optimal borehole stability and operation.

## INTRODUCTION

Swelling and overpressuring of shales are of major importance in the oil industry where, if uncontrolled, they may cause extensive damage in the form of land slides, unstable constructions, blow-outs, collapse of boreholes, sticking of drillpipes, and even loss of borehole direction. These phenomena are associated with changes in clay mineralogy during compaction and burial diagenesis, reactions with pore fluids and brines, and, in boreholes, reactions with drilling muds. In addition, migration of fluids along with chemical potential, osmotic, or pressure gradients also contribute to swelling and overpressuring.

Clay minerals in mudrocks located in the limit between the zones of early and intense diagenesis, where the burial temperature is about 80°C, are subjected to transformations that are essentially associated with the surface properties of the clay minerals, different from those transformations occurring in the deeper zone of intense diagenesis, where burial temperatures are in the range 80-120°C, and which affect the structure of the minerals. In the zone of early diagenesis cation adsorption and exchange and hydration of smectites are predominant. Most of the studies done on the adsorption of cations have involved well-selected homoionic monomineralic montmorillonite species (Pezerat and Mering, 1967; Mamy, 1968; Tarasevich and Ovcharenko, 1975; Newman, 1987; Berend, 1991; Cases et al., 1997), as opposed to rare studies on the adsorption of cations on smectitic shales and the effect of adsorption on swelling and stability at burial temperatures greater than ambient conditions. This paper reports the results of an examination of cation adsorption on shale and discusses its effects on clay mineralogy and swelling of Oligocene clay sediments from the Southern Gulf of Mexico.

Burial diagenesis of clay sediments has been known for sediments from the Northern Gulf of Mexico, which are Miocene and Pliocene. They consist predominantly of mixed-layer illite-smectite that transforms to illite with increasing depth (Burst, 1969; Shutov et al., 1969; Hower, 1981; Perry and Hower, 1970; Hower et al., 1976; Freed and Peacor, 1989; Eberl, 1993; Rask et al., 1997). Similar studies have been published on the mudrocks and sandstones of the North Sea (Berner, 1984; Pearson and Small, 1988; Hall, 1993; Primmer et al., 1993; Bjorlykke, 1998) and their clay minerals (Saas et al., 1987; Rae et al., 1993; Small and Manning, 1993; Primmer et al., 1993). Smectite under wetting and

drying conditions weathers to illite or illite-smectite, chlorite, and quartz (Perry and Hower, 1970; Mamy and Gaultier, 1975; Hower et al., 1976; Walker et al., 1978; Boles and Francks, 1979; Srodon and Eberl, 1984). Illitization may also occur via dissolution and precipitation (Altaner and Ylagan, 1997). In contrast, the sediments from the Southern Gulf of Mexico have not been described. This report considers Oligocene sediments from a depth where the burial temperature is 80°C. Diagenesis and illitization have not proceeded to a large extent and the clay minerals, which represent a large proportion of the sediment, are smectite and mixed-layer illite-smectites.

Published studies on swelling have dealt preferentially with adsorption of single cations on montmorillonites, correlating the changes in their *d*(00l)-values with the adsorbed cations, their hydration, and the charge on the clay surface (Tarasevich and Ovcharenko, 1975; Ormerod and Newman, 1983; Ben-Brahim *et al*., 1986; Berend, 1991; Berend *et al*., 1995; Cases *et al*., 1992, 1997). The adsorption of divalent cations of high hydration energy, such as $Ca^{2+}$ and $Mg^{2+}$, develops two-water layer montmorillonite complexes, whereas monovalent cations of lower hydration energy such as $Na^{+}$ and $K^{+}$ form one-water layer montmorillonite (Tarasevich and Ovcharenko, 1975). Detailed studies on the hydration of Ca-rich montmorillonite have reported spacings of 9.55 Å when dry, 12.07-12.50 Å for one-water layer montmorillonite and 15.15 to 15.6 Å for two-water layer montmorillonite (Berend, 1991; Cases *et al*., 1997). At relative water pressures $P_{H2O}/P_o$ between 0.35-0.87, Ca-rich montmorillonite hydrates to the two-water layer of 15-15.5 Å spacing (Ormerod and Newman, 1983). Mg-rich montmorillonite is characterized in the dry state by a 10.6 Å spacing which hydrates to one-water layer of 12.1 Å and to two-water layers of 14.0, 14.75, and 15.9 Å spacings. The *d*(001)-values increase in the order Ca > Sr > Ba > Mg (Cases *et al*., 1997). The adsorption of alkaline cations on montmorillonite develops Na-rich montmorillonite of characteristic 9.70 Å spacing when dry, 11.79 Å at a relative water pressure of 0.45, and 12.08 Å at a relative water pressure of 0.95. For K-rich montmorillonite the spacings are 10.12 Å dry, 11.31 Å upon hydration at $P_{H2O}/P_o$ between 0.4-0.6, and 15.76 A at relative water pressures of 0.95 (Berend *et al*., 1995). Desorption of two-water layer montmorillonite leads to a large proportion of a one-water layer phase and a small proportion of the zero-layer water montmorillonite (Ben-Brahim *et al*., 1986). The trend to form two-water layer montmorillonite increases with the hydration energy of the exchangeable cations in the order Cs > Rb > Na > K > Na > Ca > Mg; at 30°C, adsorption of $H_2O$ and swelling depend on the solvation energy of the cation (Cases *et al*., 1992, 1997).

The organization of the $H_2O$ molecules on the clay surface and in the interlamellar space of montmorillonite in different hydrated states appears to be controversial (Del Pennino *et al*., 1981; Moore and Hower, 1986; Cases *et al*., 1992, 1997; Berend *et al*., 1995). One-water layer montmorillonite with monovalent cations consists of $H_2O$ molecules arranged in an ice-like configuration (Pezerat and Mering, 1967; Mamy, 1968; Ben-Brahim *et al*., 1986) but one-water layer montmorillonite saturated with calcium can not form, possibly because of the strong solvating energy of the cation (Mamy, 1968). Monte Carlo simulation methods were applied to study hydration and adsorption of cations on montmorillonite at 300 K kipper *et al*., 1993). For Mg-rich montmorillonite, *d*(001)-values of 11.1, 14.1, and 14.7 Å for water contents respectively of 0, 100, and 200 mg/g were computed, which compare favorably with the 11.2, 14.4, and 14.6 Å spacings measured experimentally for Mg-rich smectite. For Na-rich montmorillonite, the calculated spacings are 9.8, 11.9, and 14.2 Å (Skipper *et al*., 1993). They are 9.7, 12.0, 15.5, and 18.3 Å for water/clay ratios of 43, 108, 186, and 223 mg $H_2O$/mg (Karaborni *et al*., 1996) vs. experimental values of 9.8, 12.4, and 15.2 Å (Suquet *et al*., 1975).

These adsorption and simulation studies were largely performed on well-characterized montmorillonites adsorbing single cations at near room temperature. They define characteristic *d*(00l)-values for cation-saturated montmorillonites hydrated under established water vapor partial pressures that may not necessarily occur at burial conditions. Other studies showed that smectite weathers to illite, chlorite, and quartz or to possibly dehydrated interstratifications of 17-, 14-, and 10-Å spacings (Srodon and Eberl, 1984). Consequently, it is questioned whether at burial conditions the stable forms and transformations are between water saturated smectites and should be interpreted as such, or whether they are between mixed-layer interstratifications of nearly similar characteristic spacings which may have different behavior. When *in situ* conditions of temperature and pressure are applied, then the progressive illitization of smectite with depth of burial and those transformations which are related to cation adsorption and hydration of the clay surface may modify the stability of the shale without necessarily changing its mineralogy. Not many studies (Aplin, 1993) have dealt with adsorption in shales, which may have complex clay mineralogy, different adsorbed species, or exposure to different fluids at *in situ* burial conditions of temperature and pressure. The present paper characterizes the clay mineralogy of Oligocene shale from the Southern Gulf of Mexico, describing the effects of cation adsorption, exchange, and hydration on the transformations and swelling that may occur at a surface temperature of

22°C and at a burial temperature of 80°C, and their application to the modeling of drilling muds that would maintain maximum stability in the borehole.

## METHODOLOGY

Oligocene shale from the Southern Gulf of Mexico, cored between depths from 2464.9 to 2465.8 m was analyzed to produce the data presented in this paper (see Table 1). The core samples for study were kept covered with reversed emulsion drilling fluid in closed aluminum containers. They did not require any treatment other than washing with xylene to remove the drilling fluid. Shale was analyzed using optical microscopy on thin sections and by oil-immersion to identify the coarse grained minerals and their textural relations. The clay minerals were identified by using oriented mineral aggregates and by X-ray diffraction (XRD) of air-dry, wet, and glycolated specimens. A Siemens D5000 diffractometer, filtered CuK$\alpha$ radiation, scanning at a rate 1 °2$\theta$/min from 2 to 65 °2$\theta$ and at 0.5 °2$\theta$/min from 2 to 15 °2$\theta$ was used. The microtextural relations and morphology of the clay were studied by scanning electron microscopy (SEM) coupled to energy dispersive X-ray (EDX) spectrometry. Quantitative mineral analysis of the shale was performed by XRD. The <2 $\mu$m and <0.5 $\mu$m-size fractions were extracted by settling and analyzed by X-ray analyses. The cation exchange capacity (CEC) of the shale was determined by extraction with ammonium acetate. Soluble minerals, particularly halite, estimated to represent 1 wt. % of the shale (see Table 1), released Na which increased the CEC, even after thoroughly washing the sampled material prior to the analysis of the CEC.

To analyze the effect of water, bulk shale was dried to 60°C and pulverized to –140 mesh. The shale was rehydrated at 22 and 80°C for periods of 30 and 60 min while maintaining the shale/water ratio at 1/10. The hydrated shale was subsequently reacted with solutions of 0.0001M and 0.001M $Na^+$, $K^+$, $Ca^{2+}$, and $Mg^{2+}$ chlorides to asses the cation adsorption and effects on the clay mineralogy, including mineral stability. The adsorption experiments were conducted in 30-$cm^3$ Teflon containers enclosed in static stainless steel pressure vessels. The shale/electrolyte solution ratio was maintained at 1/10. The reactions were for successive periods of 30 or 60 min, each sample reacted for 30, 60, and 90 min or 60, 120, and 180 min, at 22°C and at the burial temperature of 80°C. The equilibrium pressures at these temperatures are respectively 0.027 and 0.482 atm, far below the *in situ* burial lithostatic pressure prevailing at the depth of 2465 m. At these conditions of reaction, the clay minerals can be fully hydrated and any transformation will be associated with their surface, interlamellar spacing, or layer stacking, without affecting the layers themselves or their structure. The reactions were monitored at intervals of 30 min until reaching 180 or 240 min, while increasing the electrolyte concentration. After reaction, the solutions were decanted and analyzed by atomic absorption and flame spectrometry for Ca, Mg, Na, and K, calculating by difference the adsorbed cations. The wet, solid residue was pipetted and deposited on glass slides for XRD analysis. The remaining solid residue was again dispersed in new electrolyte solution, with a 1/10 ratio, placed in the pressure vessel, and reacted for another equal period of time and temperature. The reacted shale was washed with water to remove any excess of cations and to assess the effect of water on the newly formed smectites. Samples for diffraction were not washed. The diffractograms were obtained on wet, air-dry, and glycolated material at room conditions. The diffractograms were smoothed and background corrected; all figures shown use the same intensity scale, 0-70 counts/s. Mixed-layer interstratifications were simulated using the NEWMOD software (Reynolds and Reynolds, 1996). The transfer of cations between electrolyte solutions and shale is discussed in terms of the activity coefficients of the solutions. The activity coefficients of the reactant electrolyte solutions were calculated from the Debye-Huckel theory using the method and ionic radii in aqueous solutions at 25°C reported by Dean (1985).

## RESULTS

### Adsorption studies

The experimental data on cation adsorption are presented in Table 2. The exchangeable cations in the bulk shale in meq/100 g are 43.45 Na, 0.85 K, 31.54 Ca, and 7.94 Mg. Leaching with water reduces these values to 26.70 Na meq/100 g, 0.85 K, 30.93 Ca, and 7.78 Mg (average of tests series AO in Table 2), removing 40.6% of the absorbed Na, 1.7% Ca, 1.7% Mg and none of the K (Figure 1). The large reduction in the adsorbed Na is attributed to halite dissolved from the bulk shale.

Reaction at 22°C between the rehydrated shale and 0.0001M NaCl solution (Table 2) removes from the shale 23.1% of the initial Na, 14.34% Mg and essentially none of the K and Ca. At 80°C the trend

continues and 17% Na and 2.33% Mg are leached after a 120 min reaction. Increasing the reaction time to 240 min doubles the Na removed. Where the concentration of the electrolyte is 0.001M Na, comparable concentrations of Na and Mg, minor Ca and none of the K are removed from the rehydrated shale. The data indicate that Na in the shale decreases and is not transferred from the solution to the shale even when in contact with concentrated 0.001M NaCl electrolyte.

Reaction between the rehydrated shale and KCl solutions produces similar results (Table 2). Na and Mg are removed at near equal levels that by the NaCl solution, and Ca is scarcely leached by concentrated K solution. However, K is readily transferred from concentrated 0.001M KCl to the shale which raises its content of K by 254% of the initial value of the shale. In a similar manner, Ca and Mg concentrated electrolytes react with the hydrated shale by transferring Ca and Mg to the shale. (Table 2).

The data indicate that as the concentration of an electrolyte solution increases or its activity coefficient is reduced, the adsorption of K, Ca, or Mg by the shale increases but not that of Na which is removed to the solution (Table 2, Figure 1). This is attributed to soluble halite or excess Na in the shale relative to the Na electrolyte solution. Alternatively, the activity coefficient of Na in the shale is lower than that in the solution.

**X-ray diffraction**

The clay minerals in the shale are characterized using the criteria below.

*Illitic material I*. I is referred to in this report to the non-expandable 2:1 phyllosilicate with an intense 9.92-10.10-Å reflection, that is transformed to or formed from mixed layer illite-smectite. It could be termed illite in the sense that it is non-expandable, detrital or authigenic, primarily with K as the interlayer cation (Bailey, 1986). However, the term illitic material is preferred in this report on account of its ready cation exchangeability, adsorption, hydration, and instability (Gaudette *et al*., 1966; Srodon and Eberl, 1984). It may easily be mistaken by illite-smectite interstratifications of 0.9-0.95 illite content which develop a 10.2-Å spacing (Reynolds and Reynolds, 1996) or by dry Na-, Ca-, and Mg-rich montmorillonites which have *d*(001)-values below 9.9 Å (Suquet *et al*., 1975; Berend, 1991; Skipper *et al*., 1993; Karaborni *et al*., 1996; Cases *et al*., 1997).

*Mixed-layer illite-smectite*. The interstratifications of illite-smectite are recognized in three forms: (1) I(0.5-0.9)-S R 0. Random illite-smectite, varying from 0.5 to 0.9 I with (Riechweite) R 0. It is characterized by an intense reflection between 13.00-13.82 Å or from 10.32 to 10.28 Å, depending on the content of illite. Upon glycolation, the *d*-values of the intense reflection shift to 16.38-17.10 Å, and a less intense reflection occurs at 8.58-9.82 Å. Values near 8.58 Å represent low-illite interstratifications whereas those close to 9.82 Å correspond to smectite-rich stratifications; (2) I(0.5)-S R 1. Ordered illite-smectite, with 0.5 I and R 1, represented by reflections between 12.19-12.53 Å when dried and between 12.82-13.16 Å when glycolated. These spacings coincide with those of one-water layer Na-, Ca-, and Mg-montmorillonite which are fully expandable with glycol (Suquet *et al*., 1975; Berend, 1991; Skipper *et al*., 1993; Karaborni *et al*., 1996; Cases *et al*., 1997); (3) ISII R 3. Illite(0.75-0.85)-smectite, with R 3, ISII showing characteristic reflections in the range from 11.11 to 11.79 Å (Moore and Reynolds, 1997). The spacings can be mistaken with those of Na- and K-rich montmorillonite hydrated at relatively low partial water pressures (Berend *et al*., 1995) and which are fully expandable with glycol. The diffractograms that characterize these interstratifications were simulated from the NEWMOD software (Reynolds and Reynolds, 1996).

*Mixed-layer chlorite-smectite C(0.5-0.9)-S R 0*. This mineral component is chlorite(0.5-0.9)-smectite, with R 0. Chlorite content 0.9 predominates the component. It is characterized by a second-order reflection between 7.09-7.30 Å and a first-order reflection between 14.10-14.95 Å that shifts upon glycolation to 15.80 Å (calculated) when the chlorite content is 0.5 and to 14.92 Å when C=0.8. It is differentiated from chlorite by the displacement of the (001) reflection upon glycolation and from odinite by the intensity of the ~7.1 Å (002) reflection, which in Mg-rich chlorite is weaker than its (001) peak and in Fe-rich chlorite is stronger. Two-water layer Mg-rich montmorillonite has characteristic spacings within this same range (Cases *et al*., 1997).

*Chlorite C*. C is represented by reflections between 14.10-14.95 Å and from 7.10 to 7.30 Å that are not shifted upon solvating by ethylene glycol. The intensity of the (002) reflection (Mg-rich varieties) normally is lower than that of the (001) reflection, as opposed to the Fe-rich chlorites which show (002) more intense than (001).

*Odinite Od*. Od was defined as a dioctahedral-trioctahedral 1:1 serpentine-like mineral, identified in sediments from the North Sea (Bailey, 1988; Odin, 1990; Aplin, 1993). In the present study the term odinite, Od, is applied to the non-expandable clay material characterized by an intense 7.1-7.3-Å reflection. Its formation appears to be enhanced by Mg exchange between mixed-layer illite-smectite and electrolytes. In can be easily mistaken for Fe-rich chlorite.

*Smectite S*. S shows a relatively intense reflection at 15-15.5 Å that upon glycolation shifts to 17.3-17.8 Å. Smectite is generally the two-water layer dioctahedral montmorillonite variety. Other reflections ~15, 14, 12, and 10 Å may correspond with those of partially water-saturated and dry cation-rich montmorillonite at room temperature; they fully expand with glycol (Ormerod and Newman, 1983; Berend *et al*., 1995; Cases *et al*., 1997). The spacings between 16.89-17.20 Å may correspond to glycolated smectite and to glycolated random illite-smectite (Srodon and Eberl, 1984; Reynolds and Reynolds, 1996).

The clay fraction of the bulk shale contains dioctahedral S, I, I(0.6)-S R 0, I(0.5)-S R 1, ISII, C(0.9)-S R 0, C and Od (Figure 2). The relative abundance of these minerals varies with depth. The rehydration of the bulk shale at 22°C (Figure 3A) formed some Od. At 80°C, I(0.5)-S R 0 was partially transformed to I(0.5)-S R 1. I and Od were also formed (Figure 3B and 3C). Bulk shale rehydrated for 30 or 60 min at 22°C and reacted with 0.0001M Na was almost totally transformed to fully hydrated two-water layer smectite (Figure 4A) which, when glycolated, showed a peak shift to 17.22 Å. The 7.2-Å reflection significantly reduced its intensity and did not shift upon solvating. Treatment with K solutions (Figures 4B) formed I(0.5)-S R 0, C(0.9)-S R 0, I, and Od; reflections at 13.96 and 13.18 Å correspond with illite-smectite interstratifications of different illite content. Treatment with Ca solutions (Figures 4C) formed I(0.5)-S R 0, and treatment with Mg solutions (Figure 4D) caused I(0.5)-S R 0, C(0.9)-S R 0, and minor Od to develop.

Rehydrated shale which has been submerged at 80°C in 0.0001 M solutions of all cations (Figure 5) reacts substantially different than when treated at 22°C. Reaction with Na produced S, C(0.9)-S R 0, I(0.5)-S R 0, ISII, C, I, and Od (Figure 5A and 5E). With K solutions the reaction was similar to that with Na but I and Od were significantly more abundant (Figure 5B and 5F). Reaction with Ca developed I(0.5)-S R 0 predominant to I(0.5)-S R 1, ISII, Od, and I (Figure 5C and 5G). With Mg solution the dominant phases were I, Od, C(0.9)-S R 0, and C (Figure 5D and 5H).

When the reactions at 80° were held for longer periods, the transformations of the smectite interstratifications were more intense (Figure 6). Reaction with 0.0001M Na developed I(0.5)-S R 1, I(0.5)-S R 0, ISII, minor I, and Od (Figure 6A). With K, Od and I increased appreciably over I(0.5)-S R 1, C(0.9)-S, and S (Figure 6B). Ca formed I(0.5)-S R 1 only partially from I(0.5)-S R 0, plus C(0.9)-S R 0, ISII, minor I and Od (Figure 6C) and Mg treatment resulted in I(0.5)-S R 1, I(0.5)-S R 0, C(0.5)-S R 0, ISII, S, Od, and I. The final washing of these cation-containing shales resulted in substantial formation of I and Od while reducing the contents of I(0.5)-S R 1, I(0.5)-S R 0, and C(0.9)-S R 0 (Figure 6F, 6E, 6G, and 6H).

Reaction at 80°C between rehydrated shale and concentrated 0.001M electrolytes (Figure 7) developed a mineral suite predominated by I(0.5)-S R 1 associated with I(0.5)-S R 0, C(0.9)-S R 0, and ISII. When Ca or Mg was the reacting electrolyte, the 14.5-Å reflection of C(0.9)-S or of two-water layer Ca- or Mg-rich montmorillonite became more evident. Additional hydration (Figure 8) increased the relative abundance of I and Od over I(0.5)-S R 1, I(0.5)-S R 0, and C(0.9)-S R 0 nterstratifications.

**Modeling the osmotic swelling pressure and borehole stresses**

The preceeding data was examined in terms of the double-layer theory to produce a first model to estimate the osmotic pressure of swelling. The model assumed that the clay minerals (smectite, chlorite, illitic material, and illite-smectite and chlorite-smectite interstratifications) have an overall constant surface charge represented by the CEC of the shale. The repulsion pressure, repulsion-attraction energy, and osmotic pressure were calculated for a constant clay surface charge. The pressure depends on the salinity of the fluid in contact with the clay. Other required data were the active electrolyte component, depth and temperature of formation, and the molecular weight of the clay which was calculated from SEM data. The model computed the thickness of adsorbed layer, electrostatic potential and charge density of condensed layer, charge density of difuse layer, electrostatic potential of active surface, potential drop across the adsorbed layer, potential in the middle plane, pressure of repulsion, energy of repulsion between surfaces, energy of attraction, and osmotic pressure. These data were incorporated with data on the borehole (diameter, inclination), drilling mud (specific heat, density,

electrolytes, entrance temperature, flow), and formation (ionic activity of pore fluid, specific heat, expansion coefficient, compressibility, conductivity, density, pressure). The model computed the Poisson's ratio, Young's, compressibility, rigidity, and volume modulus, compressive and tension strength, temperature effect, stresses in the borehole, and the Mohr-Coulomb fault criteria.

A series of plots were produced. Those presented illustrate the variation vs. the salinity of the fluid of the middle plane potential (Figure 9A), repulsion pressure (Figure 9B), adsorbed counterions (Figure 9C), and limiting and real stresses (Figure 9D).

## DISCUSSION

Bulk shale leached at 22 and 80°C with water for periods of 30 and 60 min decreased its adsorbed cations by an equivalent of 38.55% Na, 1.93% Ca, 3.02% Mg, and 0% K. This loss of Na is attributed to significant soluble halite in the shale. When the shale was rehydrated at 80°C, the increase of I, Od, and I(0.5)-S R 1 relative to C(0.9)-S and I(0.5)-S R 0 in the bulk shale indicates that water modified the illite-smectite interstratification from random to ordered and rearranged the distribution of cations to form I and Od. The high $H_2O$/shale ratio of 10 to 1 maintained in these reactions did not result in the full formation of one- or two-water layer smectite. Hydration shifted the *d*(00l)-values from predominant ~13.1 Å to 12.15, 10, and 7.3 Å.

Hydrated shale submerged at 22°C in weak 0.0001M Na, K, Ca, or Mg solutions transferred from 15.76 to 36.67% of the initial Na in the shale to the electrolyte solutions (see Table 2). Under the same conditions, K was not transferred, less than 0.16% Ca was, and between 10.0 and 14.3% of the Mg in the shale was displaced towards the solutions. Submersion in concentrated 0.001M solutions had oppose effects, 254.1% K was transferred from the 0.001M K solution to the shale, 18.7% Ca from the 0.001M Ca solution, and 69.3% Mg from the 0.001M Mg solution, whereas 0% Na was removed from the Na solution to the shale. The data confirm a higher concentration of Na in the shale or the dissolution of associated halite, transfer of K, Ca, and Mg from the shale to weak electrolyte solutions (activity coefficient 0.99) and, opposedly, from concentrated electrolyte solutions (activity coefficient 0.97) to the shale. The reactions transformed IS, CS, I, S, and Od from the hydrated shale to two-water layer Na-rich smectite when the electrolyte was Na, with some possibility of additional C(0.9)-S R 0 and I(0.5)-S R 0. With K solution, the reaction was to C(0.9)-S R 0, I(0.5)-S R 0, and minor I and Od. With Ca was to I(0.5)-S R 1, and with Mg to I(0.5)-S R 0 plus C(0.9)-S.

Hydrated shale reacted at 80°C with weak 0.0001M Na, K, Ca, or Mg electrolytes by the loss of 9.6% to 28.1% Na. The transformations in the illite-smectite interstratifications were different from those at 22°C. In Na solutions, S, C(0.9)-S R 0, I(0.5)-S R 0, ISII, I, and Od prevailed. Shale adsorbed 35.2% K from the K electrolyte to form I, Od, less I(0.5)-S R 1, and more C(0.9)-S. For Ca, only 1.6% Ca was removed from the solution by the shale, forming I(0.5)-S R 0 as the most abundant interstratification. In Mg electrolyte the shale adsorbed 7.0% Mg to form predominant I, Od, and C(0.9)-S R 0. When the reactions between the hydrated shale and the weak electrolytes were held for longer times, the illite-smectite interstratifications changed from random to ordered. When K was the reacting electrolyte abundant I and Od were associated with I(0.5)-S R 1. When it was Ca, I(0.5)-S R 1 was not fully transformed from I(0.5)-S R 0 and, when Mg, C(0.9)-S R 0, I(0.5)-S R 1, S, Od and I predominated.

If the reactions at 80° involved concentrated 0.001M electrolytes, reaction with 0.001M Na formed prevailing I(0.5)-S R 1 interstratification. Reaction with 0.001M K solution added 195.3% K to the shale, without forming I. Reaction with 0.001M Ca solution added 14.1% Ca to the shale and maintained the same trend of I(0.5)-S R 1, I(0.5)-S R 0, and C(0.9)-S R 0. Reaction with 0.001M Mg added to the shale 75.4% Mg to form C(0.9)-S R 0 and I(0.5)-S R 0. The final washing of these cation-saturated shales removed only very minor amounts of adsorbed cations, but $H_2O$ shifted ordered interstratifications to random and developed I and Od from ordered I-S and C-S interstratifications in the precursor cation saturated shales.

## CONCLUSIONS

Shale containing 50.8% clay minerals in the form of dioctahedral smectite, random and ordered illite(0.5)-smectite, illite(0.75)-smectite, random chlorite(0.9)-smectite, chlorite, illitic material, and odinite, reacts with $H_2O$ by losing Na and Mg. Rehydrated shale loses Na even when in contact with NaCl electrolyte solutions of 0.97 activity coefficient. When rehydrated shale is submerged in K, Ca, or Mg 0.0001M weak electrolyte solutions of high coefficient of activity (0.99), the corresponding cations are

transferred from the shale to the solutions. When submersion is in 0.001M concentrated solutions of lower coefficient of activity (0.97), the corresponding cations are transferred from the solution to the shale.

Reaction at 22°C between rehydrated shale and Na electrolyte transforms the illite-smectite interstratifications almost completely to two-water layer smectite. With K, Ca, or Mg electrolytes, the reactions produce random illite-smectite and chlorite-smectite interstratifications, illitic material (when K is adsorbed), and odinite (when Mg is adsorbed).

Reactions at 80°C between rehydrated shale and weak 0.0001M electrolytes change the random illite-smectite interstratification to ordered illite-smectite interstratification, illitic material, and odinite. When Na is the reacting electrolyte, Na is desorbed from the hydrated shale. When it is K, the shale adsorbs K from the electrolyte solution to form ordered illite-smectite interstratification, illitic material, odinite, smectite, chlorite-smectite, and chlorite. When Ca is adsorbed, the resultant association of random and ordered illite-smectite confirms that Ca is not as efficient as Na in developing order in the illite-smectite interstratifications; Ca does not form additional illitic material and odinite. When Mg is adsorbed, Mg strengthens chlorite-smectite and develops ordered illite-smectite interstratification, odinite, and smectite.

Rehydrated shale reacting with weak 0.0001M Na, K, Ca, and Mg solutions at 80°C for 120 min formed illitic material and odinite predominant to random and ordered illite-smectite interstratifications. When the reactions lasted for 180 min, ordered illite-smectite interstratification was predominant to odinite and illitic material. It appears that, versus time, illite-smectite and chlorite-smectite interstratifications transform, initially, to illitic material plus odinite, which later reaccomodate to ordered illite-smectite interstratification and less abundant illitic material and odinite. If the reacting electrolyte is Na, ordered illite-smectite is essentially the single predominant phase. If it is K, illitic material and odinite are in about equal proportion than ordered illite-smectite interstratification. If it is Ca, ordered illite-smectite interstratification is predominant to minor illitic material and odinite. And if it is Mg, odinite is predominant to ordered illite-smectite and chlorite-smectite interstratifications, smectite, and illitic material. Final washing always transforms part of the ordered illite-smectite interstratifications to illitic material and odinite.

The reactions at 80°C between the rehydrated shale and concentrated 0.001M Na and K electrolytes fully form ordered illite-smectite interstratification. With 0.001M Ca, random and ordered illite-smectite interstratifications are associated with more abundant chlorite-smectite interstratification and, with 0.001M Mg, chlorite-smectite interstratification predominates over the random illite-smectite interstratification. In the three cases, illitic layer and odinite are not formed. Final washing produces odinite and illitic layer, apparently from precursor ordered illite-smectite and chlorite-smectite interstratifications

Electrolytes react with smectite and smectite interstratifications completely different at the temperature of 22°C and the burial temperature of 80°C. At 80°C, adsoprtion of K, Ca, and Mg improve stacking order by changing the accommodation between the illite and smectite layers and transforming random to ordered illite-smectite and chlorite-smectite interstratifications. If the coefficient of activity of the electrolyte solutions is 0.99 or >0.97, i.e., dilute solutions, the ordered structures are associated with illitic material and odinite. If it is 0.97, i.e., concentrated solutions, only the ordered interstratifications remain and illitic material and odinite are not formed. Washing these reacted shales partially separates illite and smectite layers and chlorite and smectite layers from their respective interstratifications.

Odinite is the puzzling phase in these reactions. Its intense ~7.2-Å reflection occurs associated with weak ~14.4-Å reflections that are often partially shadowed by more intense reflections from chlorite-smectite and random illite-smectite interstrafications and from smectite. Its formation is assisted by $H_2O$ and Mg. It is associated with a diminishing abundance of chlorite-smectite interstratification and with illitic material. The formation of its $Fe^{3+}$-rich 1:1 serpentine-type structure (Bailey, 1982) from precursor chlorite-smectite interstratification, by cation adsorption or exchange or by washing does not seem so readily acceptable. So, it may be possible that, in the present studies, odinite can instead correspond with Fe-rich chlorite.

The illite-smectite interstratifications could not transform to the chlorite-smectite interstratification under the present conditions of reaction. However, the data indicate that at 80°C, dilute solutions of 0.99 activity coefficient decrease the abundance of chlorite-smectite and illite-smectite interstratifications relative to a substantial formation of illitic material and odinite. With longer times, ordered illite-smectite

is predominant, associated with illitic material, odinite, chlorite-smectite, and smectite when the reaction is with K solution. When it is with Ca, illitic material and odinite are minor and, when it is with Mg, the association is with abundant odinite, chlorite-smectite, and smectite. When the reactions are with concentrated 0.001M electrolytes of 0.97 activity coefficient, ordered illite-smectite interstatification is about the single phase when reacting with Na or with K, and it is associated with random illite-smectite and chlorite-smectite interstratifications when reaction is with Ca. With Mg, the phases are chlorite-smectite and random illite-smectite interstratifications. In none of the reactions with 0.001M solutions are formed illitic material and odinite. Evidently, concentrated electrolytes Ca, Mg, Na, and K, in this order, succeed in stabilizing the smectite interstratifications but $H_2O$ easily destabilizes them. It appears that dilute electrolytes or water remove Na and Mg to transform illite-smectite and chlorite-smectite interstratifications to separate layers of illitic material and smectite and of odinite or Fe-rich chlorite and smectite respectively. Concentrated electrolytes which add cations to the shale do not form illitic material and odinite but maintain the illite-smectite and chlorite-smectite interstratifications.

The (00l) spacings change through cation adsorption and hydration. The ~13.5 Å random illite-smectite interstratification transforms to ~12.4-Å ordered illite-smectite interstratification, equivalent to a ~1.1 Å or 8.1 % contraction. With the adsorption of K, the illite-smectite interstratification partially transforms to 10.0-Å illitic material, implying a 3.5-Å or 25.9 % contraction. With Ca or Mg, the ~15.5-Å smectite and particularly the ~7.1-Å odinite increases in abundance, developing expansion and contraction respectively. When $H_2O$ is added, illitic material formed at the expense of the illite-smectite interstratifications, reducing the (00l) spacings. From a rock mechanics point of view, these changes must impinge on the stability of the shale. Possibly more significant is that these transformations are associated with depletion of electrolytes from the surrounding solutions, thus developing osmotic gradients between the clay surface and the surrounding electrolytes.

## ACKNOWLEDGMENTS

We thank I. Aguilera, M. Cruz, A. Maturano, and M. Reyes for their assistance with the analytical work, and A. Altamira for the photographic reproductions. This research was supported by Instituto Mexicano del Petróleo grant FIES 97-04-1.

## REFERENCES

Altaner, S.P. and Ylagan, R.F. (1997) Comparison of structural models of mixed-layer illite/smectite and reaction mechanisms of smectite illitization. *Clays and Clay Minerals*, **45**, 517-533.

Aplin, A. C. (1993) The composition of authigenic clay minerals in recent sediments: links to the supply of unstable reactants. In *Geochemistry of Clay-Pore Fluid Interactions*, D.A.C. Manning, P.L. Hall, and C.R. Hughes, eds., Chapman & Hall, London, 81-106.

Bailey, S.W. (1986) Report of AIPEA Nomenclature Committee (Illite. - Glauconite. - Volkonskoite). Supplement to AIPEA Newsletter 22, 1 p.

Bailey, S.W. (1988) Odinite, a new dioctahedral-trioctahedral Fe3+-rich 1:1 clay mineral. *Clay Minerals*, **23**, 237-247.

Ben-Brahim, J., Armagan, N., Besson, G., and Tchoubar, C. (1986) Méthode diffractométrique de caracterisationtion des états d'hydratation des smectites et stabilité relative des couches d'eau insérées. *Clay Minerals*, **21**, 111-124.

Berend, I. (1991) Les mécanismes d'hydratation de montmorillonites homoiniques pour des pressions relatives inférieures a 0.95, Institut National Polytechnique de Lorraine, Nancy, France, 330 pp.

Berend, I., Cases, J.M., Francois, M., Uriot, J.P., Michot, L., Masion, A., and Thomas, F. (1995) Mechanism of adsorption and desorption of water vapor by homoionic montmorillonites: 2. The $Li^+$, $Na^+$, $K^+$, $Rb^+$, and the $Cs^+$ exchanged form. *Clays and Clay Minerals*, **43**, 324-336.

Berner, R.A. (1984) Sedimentary pyrite formation: an update. *Geochimical and Cosmochimical Acta*, **8**, 324-336.

Bjorlykke, K. (1998) Clay mineral diagenesis in sedimentary basins – a key to the prediction of rock properties. Examples from the North Sea Basin. *Clay Minerals*, **33**, 15-34.

Boles, J.R. and Franks, S.G. (1979) Clay diagenesis in Wilcox sandstones of Southwest Texas: implications of smectite diagenesis on sandstone cementation. *Journal Sedimentary Petrology,* **49**, 55-70.

Burst, J.F. (1969) Diagenesis of Gulf Coast clayey sediments and its possible relation to petroleum migration. *Bulletin American Association Petroleum Geologists*, **53**, 73-93.

Cases, J.M., Bérend, I., Besson, G., Francois, M., Uriot, J.P., Thomas, F., and Poirier, J.P. (1992) Mechanisms of adsorption-desorption of water vapor by homoionic montmorillonite. 1. The sodium exchange form. *Langmuir*, **8**, 2730-2739.

Cases, J.M., Bérend, I., Francois, M., Uriot, J.P., Michot, L.J., and Thomas, F. (1997). Mechanism of adsorption and desorption of water vapor by homoionic montmorillonite: 3. The $Mg^{2+}$, $Ca^{2+}$, $Sr^{2+}$ and $Ba^{2+}$ exchanged forms. *Clays and Clay Minerals*, **45**, 8-22.

Dean, J.A. de (1985) *Lange's Handbook of Chemistry*, 13th edition, McGraw-Hill, New York, p 5.3.

Del Pennino, U., Mazzega, E., Valeri, S., Alietti, A., Brigatti, M.F., and Poppi, L. (1981) Interlayer water and swelling preperties of monoionic montmorillonites. *Journal Colloid Interface Science*, **84**, 301-309.

Eberl, D. (1993) Three zones for illite formation during burial diagenesis and metamorphism. *Clays and Clay Minerals*, **41**, 26-37.

Freed, R.L. and Peacor, D.R. (1989) Variability in the temperature of the smectite/illite reaction in Gulf Coast sediments. *Clay Minerals*, **24**, 171-180.

Gaudette, H.E., Eades, J.L., and Grim, R.E. (1966) The nature of illite. *Clays and Clay Minerals,* 12, 33-48.

Hall, P.L. (1993) Mechanisms of overpressuring: an overview. In *Geochemistry of Clay-Pore Fluid Interactions*, D.A.C. Manning, P.L. Hall, and C.R. Hughes, eds., Chapman & Hall, London, 265-315.

Hower, J. (1981) Shale diagenesis. In *Clays and the Resource Geologist*, F.T. Longstaffe, ed., Short Course Handbook 7, Mineralogical Association of Canada, Ottawa, 60-80.

Hower, J., Eslinger, E.V., Hower, M., and Perry, E.A. (1976) Mechanism of burial metamorphism of argillaceous sediments: 1. Mineralogical and chemical evidence. *Clays and Clay Minerals*, **38**, 449-468.

Karaborni, S., Smit, B., Heidug, W., Urai, J., and van Oort, E. (1996) The swelling of clays: Molecular simulations of the hydration of montmorillonite. *Science*, **271**, 1102-1104.

Mamy, J. (1968) Recherches sur l'hidratation de la motmorillonite: Propriétés diélectriques et structure du film d'eau. *Annales Agronomie*, **19**, 175-292.

Mamy, J. and Gaultier, J.P. (1975) Etude de l'evolution de l'ordre cristallin dans la montmorillonite en relation avec la diminution d'exchangeabilite du potassium. *Proccedings International Clay Conference*, Mexico City, 149-155.

Moore, D.M. and Hower, J. (1986) Ordered interstratification of dehydrated and hydrated Na-smectites. *Clays and Clay Minerals*, **34**, 379-384.

Moore, D. M. and Reynolds, R. C. (1997) *X-ray diffraction and the identification and analysis of clay minerals*. Oxford University Press, Oxford, 377 pp.

Newman, A.C.D. (1987) The interaction of clays with clay mineral surfaces. In *Chemistry of Clays and Clay Minerals*, A.C.D. Newman ed., Longman, Birmingham, Al., 237-274.

Odin, G.S. (1990) Clay mineral formation at the continent-ocean boundary: the verdine facies. *Clay Minerals*, **25**, 477-483.

Ormerod, E.C. and Newman, A.C.D. (1983) Water sorption on Ca-saturated clays: II. Internal and external surfaces of montmorillonite. *Clays and Clay Minerals*, **18**, 289-299.

Pearson, M.J. and Small, J.S. (1988) Illite-smectite diagenesis and paleotemperatures in Norhern Sea Quaternary to Mesozoic shale sequences. *Clay Minerals*, **23**, 109-132.

Perry, E. and Hower, J. (1970) Burial diagenesis in Gulf Coast pelitic sediments. *Clays and Clay Minerals*, **18**, 165-177.

Pézerat, H. and Méring, J. (1967) Recherches sur la position des cations échangeables et de l'eau dans les montmorillonites. *Comps Rendus Academy Science Paris*, **D 265**, 529-532.

Primmer, T.J., Warren, E.A., Shama, B.K., and Atkins, M.P. (1993) The stability of experimentally grown clay minerals: implications for modeling the stability of neoformed diagenetic clay minerals. In *Geochemistry of Clay-Pore Fluid Interactions*, D.A.C. Manning, P.L. Hall, and C. R. Hughes, eds., Chapman & Hall, London, 163-180.

Rae, E.Y.C., Manning, D.A.C., and Hughes, C.R. (1993) Experimental diagenesis of mudrocks. In *Geochemistry of Clay-Pore Fluid Interactions*, D.A.C. Manning, P.L. Hall, and C.R. Hughes, eds., Chapman & Hall, London, 213-242.

Rask, J.H., Bryndzia, T., Braunsdorf, N.R., and Murray, T.E. (1997) Smectite illitization in Pliocene-Age Gulf of Mexico mudrocks. *Clays and Clay Minerals*, **45**, 99-109.

Reynolds, R.C. and Reynolds, R.C.III (1996) NEWMOD. The calculation of one-dimensional X-ray diffraction patterns of mixed-layered clay minerals. R.C. Reynolds, Hanover, New Hamshire, 25 pp.

Saas, B.M., Rosenberg, P.E., and Kittrick, J.A. (1987) The stability of illite/smectite during diagenesis: an experimental study. *Geochimica et Cosmochimica Acta*, **51**, 2103-2115.

Skipper, N.T., Refson, K., and McConnell, J.D.C. (1993) Monte Carlo simulation of Mg- and Na-smectites. In *Geochemistry of Clay-Pore Fluid Interactions,* D.A.C. Manning, P.L. Hall, and C.R. Hughes, eds, Chapman & Hall, London, 40-61.

Shutov, V.D., Drits, V.A., and Sakharov, B.A. (1969) On the mechanism of a postsedimentary transformation of montmorillonite into hydromica. In *Proceedings International Clay Conference*, Tokyo, 523-532.

Small, J.S. and Manning, D.A.C. (1993) Laboratory reproduction of morphological variations in petroleum reservoir clays: monitoring of fluid composition during illite precipitation. In *Geochemistry of Clay-Pore Fluid Interactions*, D.A.C. Manning, P.L. Hall, and C.R. Hughes, eds., Chapman & Hall, London, 181-212.

Srodon, J. and Eberl, D.D. (1984) Illite. In *Reviews in Mineralogy*, S.W. Bailey, ed., Mineralogical Society of America, Washington, v. 13, 495-544.

Suquet, H,, de la Calle, C., and Pezerat, H. (1975) Swelling and structural organisation of saponite. *Clays and Clay Minerals*, **31**, 9-16.

Tarasevitch, J.I. and Ovcharenko, F.D. (1975) *Adsorption sur des Minéraux Argileux*, Naukova Dumka, Kiev, Russia, 351 pp.

Walker, T.R., Waugh, B., and Crone, A.J. (1978) Diagenesis in first-cycle desert alluvium of Cenozoic age, southwestern United States and northwestern Mexico. *Geological Society America Bulletin*, **89**, 19-32.

Table 1. Mineralogy and cation exchange capacity of Oligocene shale from the Southern Gulf of Mexico.

| Mineralogy | |
|---|---|
| quartz (%) | 20.4 |
| calcite | 17.6 |
| plagioclase | 6.3 |
| K-feldspar | 3.4 |
| halite | 1.0 |
| clay minerals | 50.8 |
| smectite dioctahedral | |
| illitic material | |
| random illite(0.6)-smectite | |
| ordered illite(0.5)-smectite | |
| illite(0.75)-smectite | |
| chlorite(0.90)-smectite | |
| chlorite | |
| odinite | |
| Cation exchange capacity (meq/100 g) | 83.12 |
| $Na^+$ | 41.18 |
| $K^+$ | 0.88 |
| $Ca^{2+}$ | 33.67 |
| $Mg^{2+}$ | 7.38 |

Table 2. Cations adsorbed by shale reacted with $Na^+$, $K^+$, $Ca^{2+}$, and $Mg^{2+}$ electrolytes.

| Sample | Electrolyte | | | | Reaction | | | Cations adsorbed (meq/100 ) | | | |
|---|---|---|---|---|---|---|---|---|---|---|---|
| | Molarity | Activity | Added (meq/100 g) | Total | Temp. (°C) | Time (min) Partial | Total | $Na^+$ | $K^+$ | $Ca^{2+}$ | $Mg^{2+}$ |
| Shale[1] | | | | | | | | 43.45 | 0.85 | 31.54 | 7.94 |
| hydrated[2] | | | | | | | | 26.70 | 0.85 | 30.93 | 7.70 |
| | | $+Na^+$ | | | | | | | | | |
| 2AO1 | 0 | 1 | 0 | 0 | 22 | 30 | 30 | 26.46 | 0.85 | 30.77 | 7.74 |
| N211 | 0.0001 | 0.9918 | 0.1 | 0.1 | 22 | 30 | 60 | 23.64 | 0.85 | 30.76 | 7.49 |
| N221 | 0.0001 | 0.9918 | 0.1 | 0.2 | 22 | 30 | 90 | 21.61 | 0.85 | 30.76 | 6.92 |
| N231 | 0.0001 | 0.9918 | 0.1 | 0.3 | 22 | 30 | 120 | 20.34 | 0.85 | 30.76 | 6.63 |
| N241 | 0 | 1 | 0 | 0.3 | 22 | 30 | 150 | 19.08 | 0.85 | 30.75 | 6.48 |
| Total %[3] | 0.0001 | 0.9918 | | 0.3 | 22 | | 120 | -23.13 | 0 | -0.03 | -14.34 |
| 2AO2 | 0 | 1 | 0 | 0 | 80 | 30 | 30 | 26.34 | 0.85 | 30.67 | 7.73 |
| N212 | 0.0001 | 0.9906 | 0.1 | 0.1 | 80 | 30 | 60 | 23.67 | 0.85 | 30.62 | 7.67 |
| N222 | 0.0001 | 0.9906 | 0.1 | 0.2 | 80 | 30 | 90 | 22.42 | 0.85 | 30.62 | 7.58 |
| N232 | 0.0001 | 0.9906 | 0.1 | 0.3 | 80 | 30 | 120 | 21.87 | 0.85 | 30.62 | 7.55 |
| N242 | 0 | 1 | 0 | 0.3 | 80 | 30 | 150 | 21.56 | 0.85 | 30.62 | 7.52 |
| Total % | 0.0001 | 0.9906 | | 0.3 | 80 | | 120 | -16.97 | 0 | -0.10 | -2.33 |
| 2AO3 | 0 | 1 | 0 | 0 | 80 | 60 | 60 | 26.76 | 0.85 | 30.96 | 7.71 |
| N213 | 0.0001 | 0.9906 | 0.1 | 0.1 | 80 | 60 | 120 | 20.31 | 0.85 | 30.83 | 7.65 |
| N223 | 0.0001 | 0.9906 | 0.1 | 0.2 | 80 | 60 | 180 | 18.15 | 0.85 | 30.83 | 7.58 |
| N233 | 0.0001 | 0.9906 | 0.1 | 0.3 | 80 | 60 | 240 | 16.96 | 0.85 | 30.81 | 7.52 |
| N243 | 0 | 1 | 0 | 0.3 | 80 | 60 | 300 | 16.21 | 0.85 | 30.77 | 7.45 |
| Total % | 0.0001 | 0.9906 | | 0.3 | 80 | | 240 | -36.62 | 0 | -0.48 | -2.46 |
| 3AO1 | 0 | 1 | 0 | 0 | 22 | 30 | 30 | 26.36 | 0.85 | 30.89 | 7.79 |
| N311 | 0.001 | 0.9754 | 1 | 1 | 22 | 30 | 60 | 22.38 | 0.85 | 30.89 | 7.59 |
| N321 | 0.001 | 0.9754 | 1 | 2 | 22 | 30 | 90 | 20.69 | 0.85 | 30.89 | 7.21 |
| N331 | 0.001 | 0.9754 | 1 | 3 | 22 | 30 | 120 | 18.71 | 0.85 | 30.85 | 6.99 |
| N341 | 0 | 1 | 0 | 3 | 22 | 30 | 150 | 17.59 | 0.85 | 30.79 | 6.91 |
| Total % | 0.001 | 0.9754 | | 3 | 22 | | 120 | -29.02 | 0 | -0.13 | -10.27 |
| 3AO2 | 0 | 1 | 0 | 0 | 80 | 30 | 30 | 26.76 | 0.85 | 31.12 | 7.89 |
| N312 | 0.001 | 0.9725 | 1 | 1 | 80 | 30 | 60 | 24.82 | 0.85 | 30.93 | 7.85 |
| N322 | 0.001 | 0.9725 | 1 | 2 | 80 | 30 | 90 | 23.49 | 0.85 | 30.71 | 7.69 |
| N332 | 0.001 | 0.9725 | 1 | 3 | 80 | 30 | 120 | 23.11 | 0.85 | 30.61 | 7.65 |
| N342 | 0 | 1 | 0 | 3 | 80 | 30 | 150 | 22.35 | 0.85 | 30.54 | 7.64 |
| Total % | 0.001 | 0.9754 | | 3 | 80 | | 120 | -13.64 | 0 | -1.64 | -3.04 |
| 3AO3 | 0 | 1 | 0 | 0 | 80 | 60 | 60 | 27.49 | 0.85 | 31.14 | 7.82 |
| N313 | 0.001 | 0.9725 | 1 | 1 | 80 | 60 | 120 | 20.83 | 0.85 | 31.08 | 7.79 |
| N323 | 0.001 | 0.9725 | 1 | 2 | 80 | 60 | 180 | 19.65 | 0.85 | 30.92 | 7.74 |
| N333 | 0.001 | 0.9725 | 1 | 3 | 80 | 60 | 240 | 18.32 | 0.85 | 30.79 | 7.61 |
| N343 | 0 | 1 | 0 | 3 | 80 | 60 | 300 | 17.72 | 0.85 | 30.69 | 7.55 |
| Total % | 0.001 | 0.9754 | | 3 | 80 | | 240 | -33.35 | 0 | -1.12 | -6.52 |
| | | $+K^+$ | | | | | | | | | |
| 2AKO1 | 0 | 1 | 0 | 0 | 22 | 30 | 30 | 24.11 | 0.85 | 30.91 | 7.73 |
| K211 | 0.0001 | 0.9918 | 0.1 | 0.1 | 22 | 30 | 60 | 22.28 | 0.95 | 30.91 | 7.31 |
| K221 | 0.0001 | 0.9918 | 0.1 | 0.2 | 22 | 30 | 90 | 21.77 | 1.05 | 30.91 | 7.11 |
| K231 | 0.0001 | 0.9918 | 0.1 | 0.3 | 22 | 30 | 120 | 20.31 | 1.15 | 30.91 | 6.91 |
| K242 | 0 | 1 | 0 | 0.3 | 22 | 30 | 150 | 20.31 | 1.15 | 30.87 | 6.82 |
| Total % | 0.0001 | 0.9918 | | 0.3 | 22 | | 120 | -15.76 | +35.29 | 0 | -10.61 |
| 2AKO2 | 0 | 1 | 0 | 0 | 80 | 30 | 30 | 22.64 | 0.85 | 30.88 | 7.77 |
| K212 | 0.0001 | 0.9906 | 0.1 | 0.1 | 80 | 30 | 60 | 20.69 | 0.95 | 30.88 | 7.67 |
| K242 | 0 | 1 | 0 | 0.2 | 80 | 30 | 120 | 20.47 | 1.15 | 30.82 | 7.54 |
| Total % | 0.0001 | 0.9906 | | 0.2 | 80 | | 120 | -9.58 | +35.24 | -0-19 | -2.96 |
| 2AKO3 | 0 | 1 | 0 | 0 | 80 | 60 | 60 | 23.04 | 0.85 | 30.96 | 7.79 |
| K213 | 0.0001 | 0.9906 | 0.1 | 0.1 | 80 | 60 | 120 | 20.96 | 0.95 | 30.96 | 7.73 |
| K223 | 0.0001 | 0.9906 | 0.1 | 0.2 | 80 | 60 | 180 | 19.62 | 1.05 | 30.95 | 7.68 |
| K233 | 0.0001 | 0.9906 | 0.1 | 0.3 | 80 | 60 | 240 | 18.94 | 1.15 | 30.93 | 7.64 |
| K243 | 0 | 1 | 0 | 0.3 | 80 | 60 | 300 | 18.71 | 1.15 | 30.92 | 7.61 |
| Total % | 0.0001 | 0.9906 | | 0.3 | 80 | | 240 | -17.79 | +35.29 | -0.09 | -1.92 |
| 3AKO1 | 0 | 1 | 0 | 0 | 22 | 30 | 30 | 26.03 | 0.85 | 31.02 | 7.78 |
| K311 | 0.001 | 0.9754 | 1 | 1 | 22 | 30 | 60 | 21.12 | 1.59 | 31.02 | 7.58 |
| K321 | 0.001 | 0.9754 | 1 | 2 | 22 | 30 | 90 | 18.57 | 2.37 | 30.96 | 7.21 |
| K331 | 0.001 | 0.9754 | 1 | 3 | 22 | 30 | 120 | 16.48 | 3.01 | 30.92 | 7.03 |

| | | | | | | | | | | | |
|---|---|---|---|---|---|---|---|---|---|---|---|
| K341 | 0 | 1 | 0 | 3 | 22 | 30 | 150 | 15.39 | 2.62 | 30.87 | 6.96 |
| Total % | 0.001 | 0.9754 | | 3 | 22 | | 120 | -36.67 | +254.12 | -0.32 | -9.64 |
| | | | | | | | | | | | |
| 3AKO2 | 0 | 1 | 0 | 0 | 80 | 30 | 30 | 24.93 | 0.85 | 31.11 | 7.87 |
| K312 | 0.001 | 0.9725 | 1 | 1 | 80 | 30 | 60 | 20.41 | 1.66 | 30.92 | 7.82 |
| K322 | 0.001 | 0.9725 | 1 | 2 | 80 | 30 | 90 | 19.11 | 2.49 | 30.86 | 7.34 |
| K332 | 0.001 | 0.9725 | 1 | 3 | 80 | 30 | 120 | 18.35 | 2.51 | 30.75 | 7.69 |
| K342 | 0 | 1 | 0 | 3 | 80 | 30 | 150 | 17.59 | 3.01 | 30.67 | 7.66 |
| Total % | 0.001 | 0.9725 | | 3 | 80 | | 120 | -26.39 | +195.29 | -1.16 | -2.29 |
| | | | | | | | | | | | |
| 3AKO3 | 0 | 1 | 0 | 0 | 80 | 60 | 60 | 26.47 | 0.85 | 31.12 | 7.86 |
| K313 | 0.001 | 0.9725 | 1 | 1 | 80 | 60 | 120 | 22.11 | 1.66 | 30.95 | 7.83 |
| K323 | 0.001 | 0.9725 | 1 | 2 | 80 | 60 | 180 | 21.23 | 2.46 | 30.84 | 7.81 |
| K333 | 0.001 | 0.9725 | 1 | 3 | 80 | 60 | 240 | 20.11 | 2.36 | 30.71 | 7.78 |
| K343 | 0 | 1 | 0 | 3 | 80 | 60 | 300 | 20.64 | 2.16 | 30.75 | 7.78 |
| Total % | 0.001 | 0.9725 | | 3 | 80 | | 240 | -24.03 | +177.64 | -1.32 | -1.02 |
| | | | | | | | | | | | |
| | | $+Ca^{2+}$ | | | | | | | | | |
| 2ACO1 | 0 | 1 | 0 | 0 | 22 | 30 | 30 | 26.03 | 0.85 | 30.96 | 7.74 |
| C211 | 0.0001 | 0.9918 | 0.2 | 0.2 | 22 | 30 | 60 | 22.87 | 0.85 | 31.15 | 7.21 |
| C221 | 0.0001 | 0.9918 | 0.2 | 0.4 | 22 | 30 | 90 | na | 0.85 | 31.36 | 6.76 |
| C231 | 0.0001 | 0.9918 | 0.2 | 0.6 | 22 | 30 | 120 | na | 0.85 | 31.55 | 6.61 |
| C241 | 0 | 1 | 0 | 0.6 | 22 | 30 | 150 | na | 0.85 | 31.54 | 6.45 |
| Total % | 0.0001 | 0.9918 | | 0.6 | 22 | | 120 | na | 0 | +1.19 | -14.60 |
| | | | | | | | | | | | |
| 2ACO2 | 0 | 1 | 0 | 0 | 80 | 30 | 30 | 27.22 | 0.85 | 31.01 | 7.79 |
| C212 | 0.0001 | 0.9906 | 0.2 | 0.2 | 80 | 30 | 60 | 21.72 | 0.85 | 31.11 | 7.75 |
| C222 | 0.0001 | 0.9906 | 0.2 | 0.4 | 80 | 30 | 90 | 20.54 | 0.85 | 31.31 | 7.66 |
| C232 | 0.0001 | 0.9906 | 0.2 | 0.6 | 80 | 30 | 120 | 20.24 | 0.85 | 31.51 | 7.58 |
| C242 | 0 | 1 | 0 | 0.6 | 80 | 30 | 150 | 19.85 | 0.85 | 31.49 | 7.54 |
| Total % | 0.0001 | 0.9906 | | 0.6 | 80 | | 120 | -25.64 | 0 | +1.61 | -2.69 |
| | | | | | | | | | | | |
| 2ACO3 | 0 | 1 | 0 | 0 | 80 | 60 | 60 | 24.79 | 0.85 | 31.15 | 7.84 |
| C213 | 0.0001 | 0.9906 | 0.2 | 0.2 | 80 | 60 | 120 | 20.55 | 0.85 | 31.28 | 7.81 |
| C223 | 0.0001 | 0.9906 | 0.2 | 0.4 | 80 | 60 | 180 | 20.35 | 0.85 | 31.48 | 7.74 |
| C233 | 0.0001 | 0.9906 | 0.2 | 0.6 | 80 | 60 | 240 | 20.05 | 0.85 | 31.66 | 7.69 |
| C243 | 0 | 1 | 0 | 0.6 | 80 | 60 | 300 | 20.05 | 0.85 | 31.65 | 7.66 |
| Total % | 0.0001 | 0.9906 | | 0.6 | 80 | | 240 | -19.12 | 0 | +1.64 | -1.91 |
| | | | | | | | | | | | |
| 3ACO3 | 0 | 1 | 0 | 0 | 22 | 30 | 30 | 26.03 | 0.85 | 31.05 | 7.82 |
| C311 | 0.001 | 0.9754 | 2 | 2 | 22 | 30 | 60 | 20.89 | 0.85 | 32.99 | 7.74 |
| C321 | 0.001 | 0.9754 | 2 | 4 | 22 | 30 | 90 | na | 0.85 | 34.95 | 7.43 |
| C331 | 0.001 | 0.9754 | 2 | 6 | 22 | 30 | 120 | na | 0.85 | 36.86 | 7.31 |
| C341 | 0 | 1 | 0 | 6 | 22 | 30 | 150 | na | 0.85 | 36.86 | 7.16 |
| Total % | 0.001 | 0.9754 | | 6 | 22 | | 120 | | 0 | +18.71 | -6.52 |
| | | | | | | | | | | | |
| 3ACO2 | 0 | 1 | 0 | 0 | 80 | 30 | 30 | 24.91 | 0.85 | 31.09 | 7.82 |
| C312 | 0.001 | 0.9725 | 2 | 2 | 80 | 30 | 60 | 20.07 | 0.85 | 32.89 | 7.76 |
| C322 | 0.001 | 0.9725 | 2 | 4 | 80 | 30 | 90 | 17.93 | 0.85 | 34.84 | 7.54 |
| C332 | 0.001 | 0.9725 | 2 | 6 | 80 | 30 | 120 | 16.74 | 0.85 | 35.57 | 7.39 |
| C342 | 0 | 1 | 0 | 6 | 80 | 30 | 150 | 15.98 | 0.85 | 36.64 | 7.33 |
| Total % | 0.001 | 0.9725 | | 6 | 80 | | 120 | -32.80 | 0 | +14.41 | -0.77 |
| | | | | | | | | | | | |
| 3ACO30 | 0 | 1 | 0 | 0 | 80 | 60 | 60 | 25.12 | 0.85 | 31.09 | 7.82 |
| C313 | 0.001 | 0.9725 | 2 | 2 | 80 | 60 | 120 | 19.77 | 0.85 | 32.87 | 7.75 |
| C323 | 0.001 | 0.9725 | 2 | 4 | 80 | 60 | 180 | 17.45 | 0.85 | 34.75 | 7.69 |
| C333 | 0.001 | 0..9725 | 2 | 6 | 80 | 60 | 240 | 16.49 | 0.85 | 36.62 | 7.59 |
| C343 | 0 | 1 | 0 | 6 | 80 | 60 | 300 | na | 0.85 | 36.51 | 7.55 |
| Total % | 0.001 | 0.9725 | | 6 | 80 | | 240 | -34.35 | 0 | +17.70 | -2.94 |
| | | | | | | | | | | | |
| | | $+Mg^{2+}$ | | | | | | | | | |
| 2AMO1 | 0 | 1 | 0 | 0 | 22 | 30 | 30 | 25.21 | 0.85 | 31.02 | 7.77 |
| M211 | 0.0001 | 0.9918 | 0.2 | 0.2 | 22 | 30 | 60 | 20.52 | 0.85 | 31.02 | 7.32 |
| M221 | 0.0001 | 0.9918 | 0.2 | 0.4 | 22 | 30 | 90 | 18.39 | 0.85 | 31.02 | 7.01 |
| M231 | 0.0001 | 0.9918 | 0.2 | 0.6 | 22 | 30 | 120 | 18.05 | 0.85 | 31.01 | 6.99 |
| M241 | 0 | 1 | 0 | 0.6 | 22 | 30 | 150 | 17.03 | 0.85 | 30.99 | 6.84 |
| Total % | 0.0001 | 0.9918 | | 0.6 | 22 | | 120 | -28.11 | 0 | 0 | -10.04 |
| | | | | | | | | | | | |
| 2AMO2 | 0 | 1 | 0 | 0 | 80 | 30 | 30 | 25.45 | 0.85 | 31.24 | 7.87 |
| M212 | 0.0001 | 0.9906 | 0.2 | 0.2 | 80 | 30 | 60 | na | 0.85 | 31.24 | 8.04 |
| M222 | 0.0001 | 0.9906 | 0.2 | 0.4 | 80 | 30 | 90 | na | 0.85 | 31.24 | 8.22 |
| M232 | 0.0001 | 0.9906 | 0.2 | 0.6 | 80 | 30 | 120 | na | 0.85 | 31.24 | 8.42 |
| M242 | 0 | 1 | 0 | 0.6 | 80 | 30 | 150 | na | 0.85 | 31.09 | 8.34 |
| Total % | 0.0001 | 0.9906 | | 0.6 | 80 | | 120 | | 0 | 0 | +6.99 |
| | | | | | | | | | | | |
| 2AMO3 | 0 | 1 | 0 | 0 | 80 | 60 | 60 | 25.45 | 0.85 | 31.03 | 7.82 |
| M213 | 0.0001 | 0.9906 | 0.2 | 0.2 | 80 | 60 | 120 | 20.15 | 0.85 | 30.92 | 7.96 |

| | | | | | | | | | | | |
|---|---|---|---|---|---|---|---|---|---|---|---|
| M223 | 0.0001 | 0.9906 | 0.2 | 0.4 | 80 | 60 | 180 | 18.78 | 0.85 | 30.85 | 8.05 |
| M233 | 0.0001 | 0.9906 | 0.2 | 0.6 | 80 | 60 | 240 | 18.31 | 0.85 | 30.82 | 8.23 |
| M243 | 0 | 1 | 0 | 0.6 | 80 | 60 | 300 | 17.91 | 0.85 | 30.77 | 8.21 |
| Total % | 0.0001 | 0.9906 | | 0.6 | 80 | | 240 | -28.05 | 0 | -0.67 | +5.24 |
| | | | | | | | | | | | |
| 3AMO1 | 0 | 1 | 0 | 0 | 22 | 30 | 30 | 26.03 | 0.85 | 30.84 | 7.79 |
| M311 | 0.001 | 0.9754 | 2 | 2 | 22 | 30 | 60 | 23.16 | 0.85 | 30.79 | 9.69 |
| M321 | 0.001 | 0.9754 | 2 | 4 | 22 | 30 | 90 | na | 0.85 | 30.79 | 11.43 |
| M331 | 0.001 | 0.9754 | 2 | 6 | 22 | 30 | 120 | na | 0.85 | 30.79 | 13.19 |
| M341 | 0 | 1 | 0 | 6 | 22 | 30 | 150 | na | 0.85 | 30.79 | 13.03 |
| Total % | 0.001 | 0.9754 | | 6 | 22 | | 120 | | 0 | -0.16 | +69.32 |
| | | | | | | | | | | | |
| 3AMO2 | 0 | 1 | 0 | 0 | 80 | 30 | 30 | 26.03 | 0.85 | 31.15 | 7.87 |
| M312 | 0.001 | 0.9725 | 2 | 2 | 80 | 30 | 60 | na | 0.85 | 30.99 | 9.84 |
| M322 | 0.001 | 0.9725 | 2 | 4 | 80 | 30 | 90 | na | 0.85 | 30.93 | 11.72 |
| M332 | 0.001 | 0.9725 | 2 | 6 | 80 | 30 | 120 | na | 0.85 | 30.85 | 13.66 |
| M342 | 0 | 1 | 0 | 6 | 80 | 30 | 150 | na | 0.85 | 30.79 | 13.61 |
| Total % | 0.001 | 0.9725 | | 6 | 80 | | 120 | | 0 | -0.96 | +75.37 |
| | | | | | | | | | | | |
| 3AMO3 | 0 | 1 | 0 | 0 | 80 | 60 | 60 | 26.03 | 0.85 | 31.15 | 7.87 |
| M313 | 0.001 | 0.9725 | 2 | 2 | 80 | 60 | 120 | 20.47 | 0.85 | 31.05 | 8.79 |
| M323 | 0.001 | 0.9725 | 2 | 4 | 80 | 60 | 180 | 21.45 | 0.85 | 30.96 | 10.56 |
| M333 | 0.001 | 0.9725 | 2 | 6 | 80 | 60 | 240 | 21.01 | 0.85 | 30.81 | 12.32 |
| M343 | 0 | 1 | 0 | 6 | 80 | 60 | 300 | na | 0.85 | 30.71 | 12.18 |
| Total % | 0.001 | 0.9725 | | 6 | 80 | | 240 | -19.28 | 0 | -1.09 | +56.54 |

---

[1]The cations adsorbed correspond with the CEC of the bulk shale.

[2]The cations adsorbed by the hydrated shale represent those remaining after leaching with water at 22 and 80°C.

[3]Total % is the percentage of cations transferred between the electrolyte and the shale with respect to the cations in the hydrated shale.

**FIGURE LEGENDS**

Figure 1. Variation of the adsorbed cations with the activity coefficient of water and the electrolyte solutions (A) NaCl solution; (B) KCl; (C) $CaCl_2$; and (D) $MgCl_2$.

Figure 2. X-ray diffractograms of the clay-size fraction of shale 2464.9-2465.8 m deep: (A) bulk; (B) glycolated. The clay fraction contains random illite(0.5-0.8)-smectite (IS), ordered illite(0.5)-smectite, illite(0.75)-smectite (ISII), chlorite (C), random chlorite(0.5)-smectite (CS), illitic material (I), smectite (S), and odinite (Od). Scanning from 2 to 15 °2θ at 0.5° 2θ/m, filtered CuKα; intensity axis is from 0 to 70 c/s.

Figure 3. X-ray diffractograms of bulk shale 2464.9-2465.8 m deep hydrated at (A) 22°C, 30 min; (B) 80°C, 60 min; (C) 80°C, 90 min. Hydrating the shale transforms the random illite-smectite interstratifications to ordered illite-smectite, illitic material, and odinite. Scanning from 2 to 15° 2θ, at 0.5 °2θ/min, filtered CuKα; intensity axis from 0 to 70 c/s.

Figure 4. X-ray data of bulk shale reacted at 22°C with (A) $H_2O$, 30 min and 0.0001M NaCl, 60 min; (B) $H_2O$, 30 min and 0.0001M KCl, 60 min; (C) $H_2O$, 30 min and 0.0001M $CaCl_2$, 60 min; (D) $H_2O$, 30 min and 0.0001M $MgCl_2$, 60 min. Weak electrolyte solutions at 22°C develop two-water layer smectite (by Na), or random illite-smectite and chlorite-smectite by other cations, associated with minor illitic material and odinite when reacting with K and odinite when reacting with Mg. Scanning from 2 to 15 °2θ, at 0.5 °2θ/min, filtered CuKα; intensity axis from 0 to 70 c/s.

Figure 5. X-ray data of bulk shale reacted at 80°C with (A) $H_2O$, 30 min and NaCl 0.0001M, 90 min; (B) $H_2O$, 30 min and KCl 0.0001M, 120 min; (C) $H_2O$, 30 min and $CaCl_2$ 0.0001M, 120 min; (D) $H_2O$, 30 min and $MgCl_2$ 0.0001M, 120 min. Diffractograms E, F, G, and H correspond with the same materials glycolated. The phases are smectite, chlorite-smectite, illite-smectite, illitic material, odinite, and chlorite in distinct proportions depending on the reacting electrolyte. Scanning from 2 to 15 °2θ, at 0.5 °2θ/min, filtered CuKα; intensity axis from 0 to 70 c/s.

Figure 6. X-ray data of bulk shale reacted at 80°C with (A) $H_2O$, 60 min and NaCl 0.0001M, 180 min; (B) $H_2O$, 60 min and KCl 0.0001M, 180 min; (C) $H_2O$, 60 min and $CaCl_2$ 0.0001M, 180 min; (D) $H_2O$, 60 min and $MgCl_2$ 0.0001M, 180 min. Following diffractograms show the effect of final washing upon cation saturated shale (E) $H_2O$, 30 min, KCl 0.0001M, 90 min and $H_2O$, 30 min; (F) $H_2O$, 60 min, NaCl 0.0001M, 180 min and $H_2O$, 60 min; (G) $H_2O$, 30 min, $CaCl_2$, 0.0001M 90 min and $H_2O$, 30 min; (H) $H_2O$, 60 min, $MgCl_2$ 0.0001M, 180 min and $H_2O$, 60 min. Reaction between water saturated shale and weak electrolytes for longer times transforms random illite-smectite interstratifications to ordered. Scanning from 2 to 15 °2θ, at 0.5 °2θ/min, filtered CuKα; intensity axis from 0 to 70 c/s.

Figure 7. X-ray data of bulk shale reacted at 80°C with (A) $H_2O$, 60 min, NaCl 0.001M, 120 min; (B) $H_2O$, 30 min, KCl 0.001M, 60 min; (C) $H_2O$, 60 min, $CaCl_2$ 0.001M, 120 min; (D) $H_2O$, 30 min, $MgCl_2$ 0.001M, 60 min. Reaction with concentrated electrolytes is to ordered illite-smectite. Scanning from 2 to 15 °2θ, at 0.5 °2θ/m, filtered CuKα; intensity axis from 0 to 70 c/s.

Figure 8. X-ray data of bulk shale reacted at 80°C with (A) $H_2O$, 30 min, NaCl 0.001M, 90 min and $H_2O$, 30 min; (B) $H_2O$, 60 min, 0.001M KCl, 180 min; (C) $H_2O$, 60 min, $CaCl_2$, 180 min and $H_2O$, 60 min. Final hydration partially transforms the illite-smectite and chlorite-smectite interstratifications to illitic material and odinite. Scanning from 2 to 15 °2θ, at 0.5 °2θ/m, filtered CuKα; intensity axis from 0 to 70 c/s.

Figure 9. Variation vs. the salinity of a calcic brine of the (A) middle plane potential; (B) repulsion pressure; (C) adsorbed counterions; (D) limiting and real stresses.

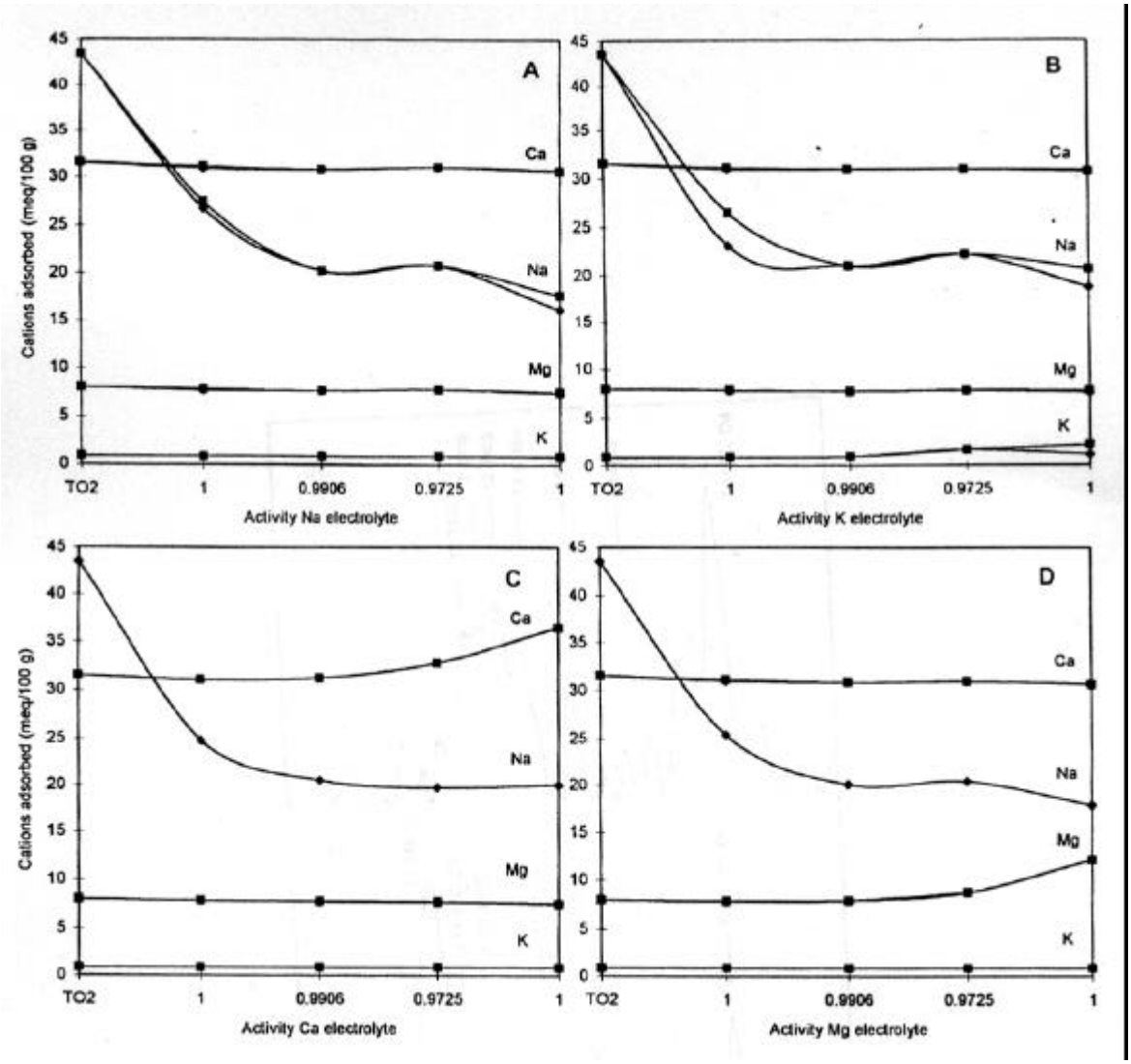
A
B
C
D
Ca
Na
Mg
K
Cations adsorbed (meq/100 g)
TO2
1
0.9906
0.9725
Activity Na electrolyte
Activity K electrolyte
Activity Ca electrolyte
Activity Mg electrolyte

**Fig. 1**

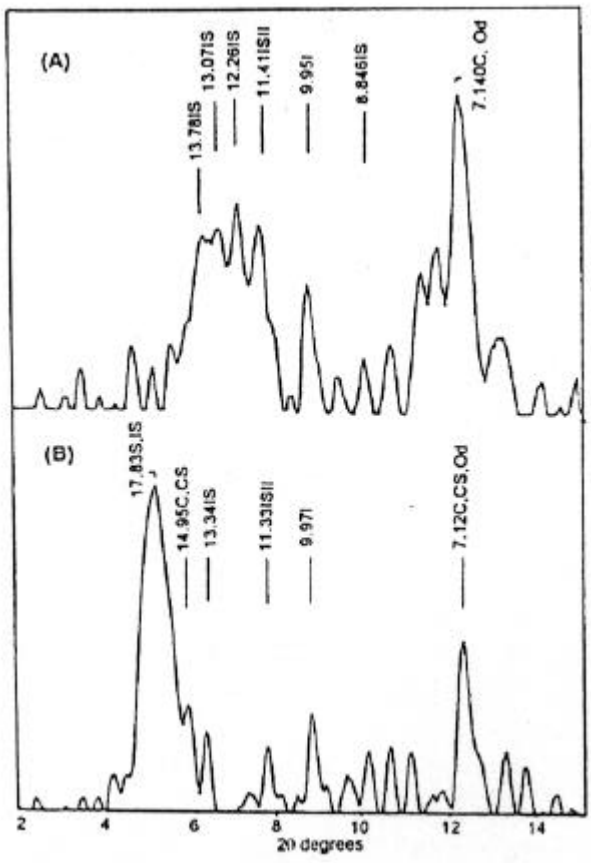
(A)
13.78IS
13.07IS
12.26IS
11.41ISII
9.95I
8.846IS
7.140C, Od
(B)
17.83S,IS
14.95C,CS
13.34IS
11.331SII
9.97I
7.12C,CS,Od
2
4
6
8
10
12
14
2θ degrees

**Fig. 2**

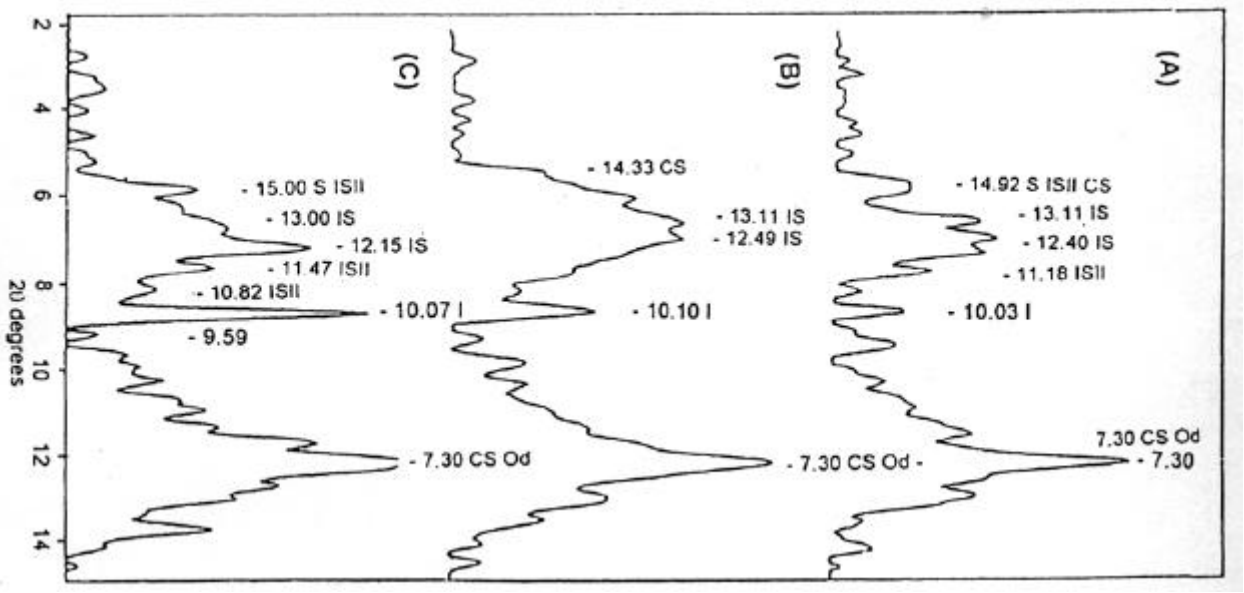
(C)
(B)
(A)
- 15.00 S ISII
- 13.00 IS
- 12.15 IS
- 11.47 ISII
- 10.82 ISII
- 10.07 I
- 9.59
- 7.30 CS Od
- 14.33 CS
- 13.11 IS
- 12.49 IS
- 10.10 I
- 7.30 CS Od -
- 14.92 S ISII CS
- 13.11 IS
- 12.40 IS
- 11.18 ISII
- 10.03 I
7.30 CS Od
- 7.30
2θ degrees
2
4
6
8
10
12
14

**Fig. 3**

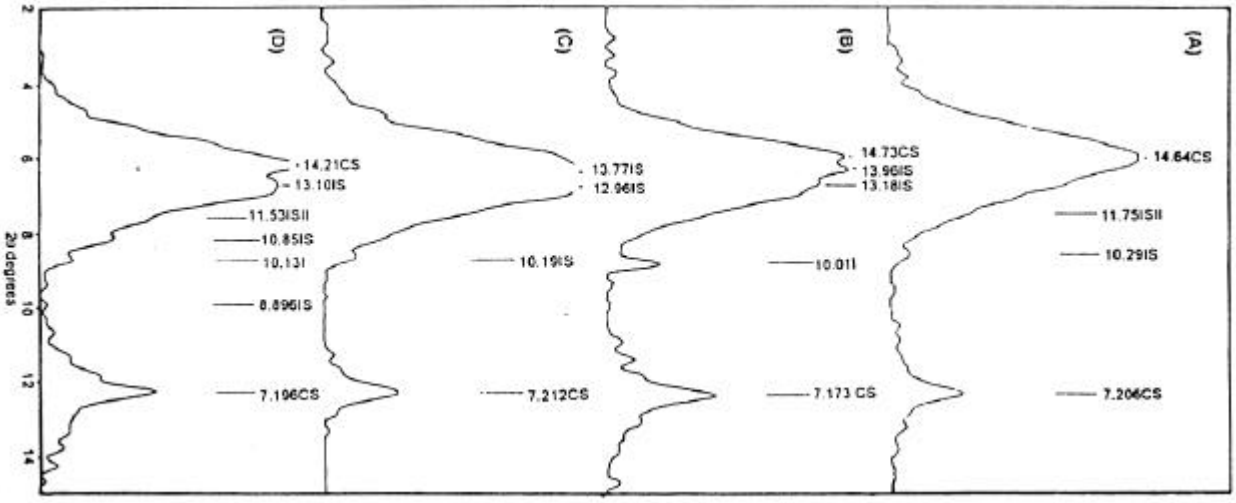
(D)
(C)
(B)
(A)
14.21CS
13.10IS
11.53ISII
10.85IS
10.13I
8.89GIS
7.196CS
13.77IS
12.96IS
10.19IS
7.212CS
14.73CS
13.96IS
13.18IS
10.01I
7.173 CS
14.64CS
11.75ISII
10.29IS
7.206CS
2θ degrees
2
4
6
8
10
12
14

**Fig. 4**

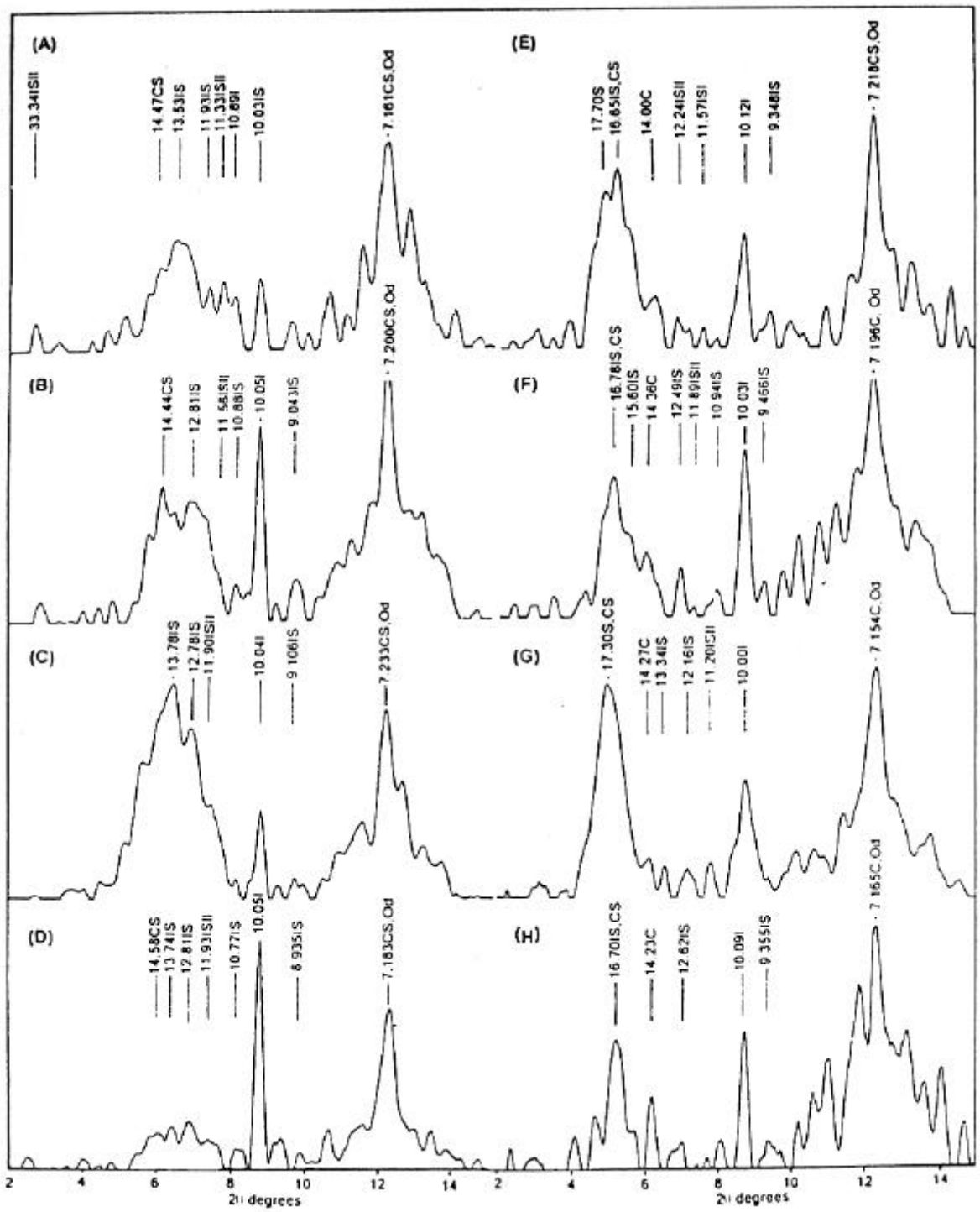
(A)
33.34ISII
14.47CS
13.53IS
11.93IS
11.33ISII
10.69I
10.03IS
7.161CS,Od
7.200CS,Od
(B)
14.44CS
12.81IS
11.58ISII
10.88IS
10.05I
9.043IS
(C)
13.78IS
12.78IS
11.90ISII
10.04I
9.106IS
7.233CS,Od
(D)
14.58CS
13.74IS
12.81IS
11.93ISII
10.77IS
10.05I
8.935IS
7.183CS,Od
(E)
17.70S
16.65IS,CS
14.00C
12.24ISII
11.57ISI
10.12I
9.348IS
7.218CS,Od
(F)
16.78IS,CS
15.60IS
14.36C
12.49IS
11.89ISII
10.94IS
10.03I
9.466IS
7.196C,Od
(G)
17.30S,CS
14.27C
13.34IS
12.16IS
11.20ISII
10.00I
7.154C,Od
(H)
16.70IS,CS
14.23C
12.62IS
10.09I
9.355IS
7.165C,Od
2 4 6 8 10 12 14
2θ degrees
2 4 6 8 10 12 14
2θ degrees

**Fig. 5**

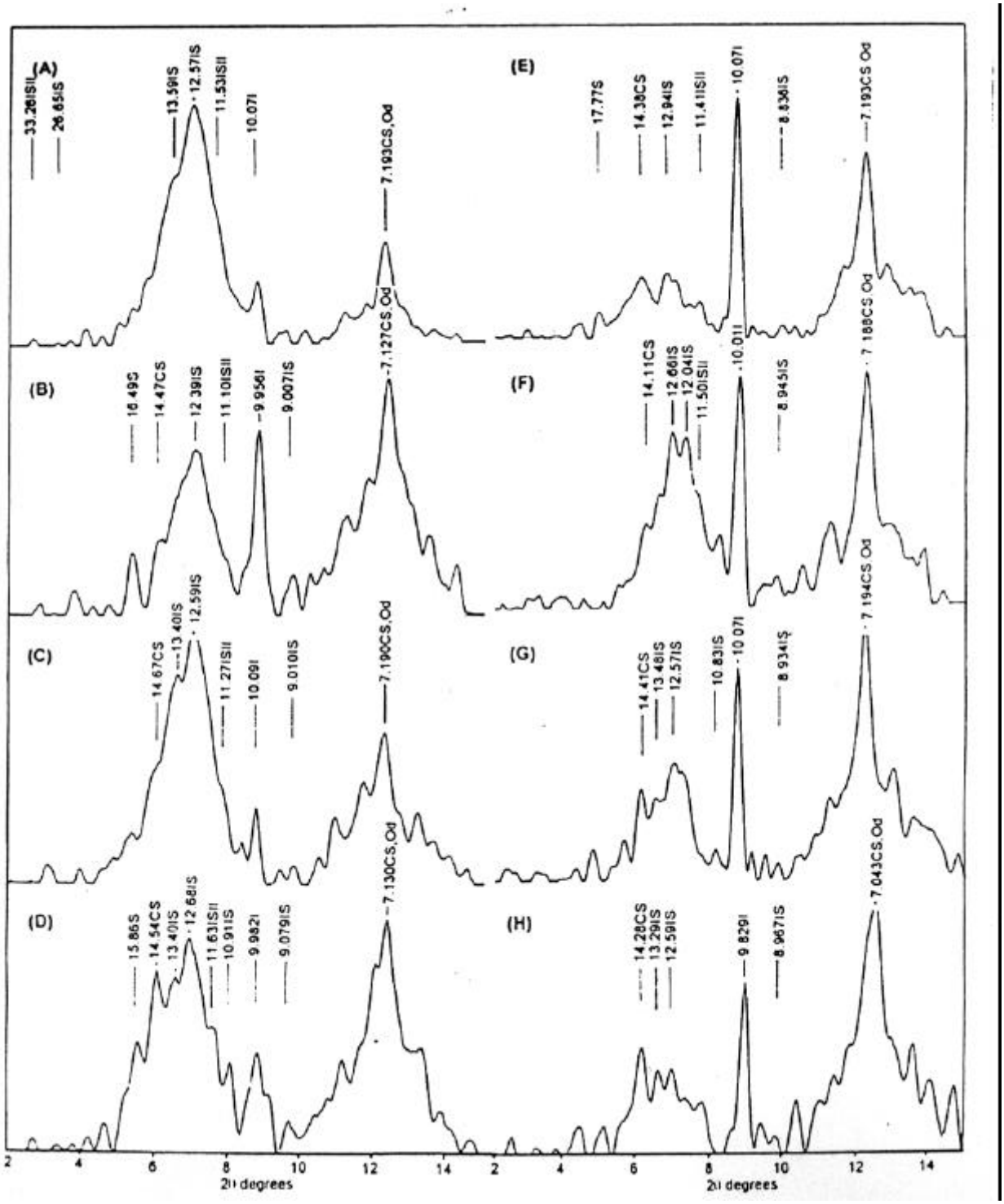
(A)
33.26ISIL
26.65IS
13.59IS
12.57IS
11.53ISII
10.07I
7.193CS,Od
(B)
16.49S
14.47CS
12.39IS
11.10ISII
9.956I
9.007IS
7.127CS,Od
(C)
14.67CS
13.40IS
12.59IS
11.27ISII
10.09I
9.010IS
7.190CS,Od
(D)
15.86S
14.54CS
13.40IS
12.68IS
11.63ISII
10.91IS
9.982I
9.079IS
7.130CS,Od
(E)
17.77S
14.38CS
12.94IS
11.41ISII
10.07I
8.836IS
7.193CS,Od
(F)
14.11CS
12.66IS
12.04IS
11.50ISII
10.01I
8.945IS
7.188CS,Od
(G)
14.41CS
13.48IS
12.57IS
10.83IS
10.07I
8.934IS
7.194CS,Od
(H)
14.28CS
13.29IS
12.59IS
9.829I
8.967IS
7.043CS,Od
2 4 6 8 10 12 14
2θ degrees
2 4 6 8 10 12 14
2θ degrees

**Fig. 6**

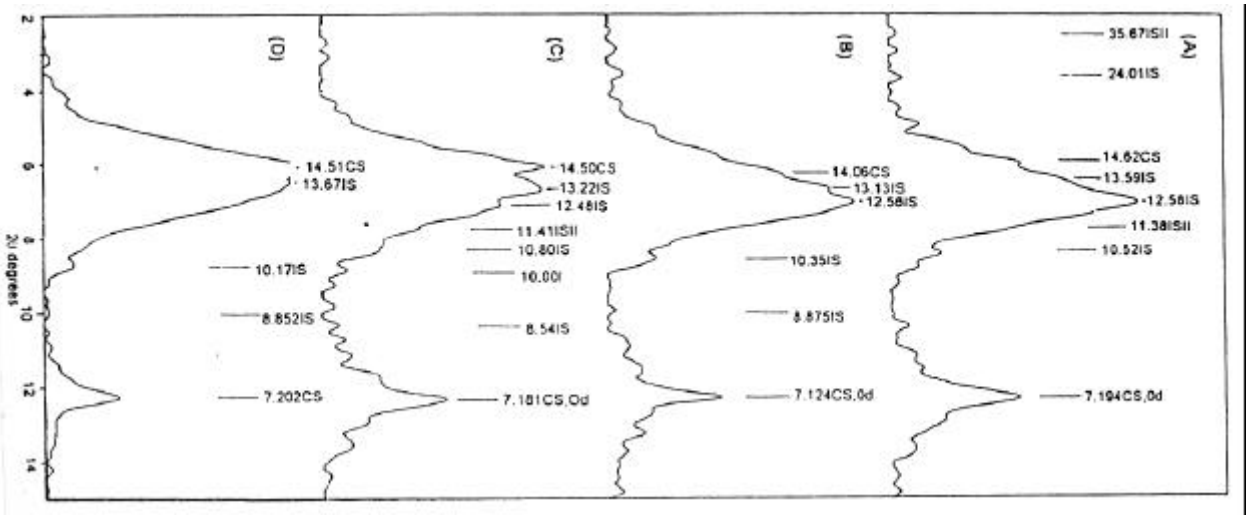
(D)
(C)
(B)
(A)
14.51CS
13.67IS
10.17IS
8.852IS
7.202CS
14.50CS
13.22IS
12.48IS
11.41ISII
10.80IS
10.00I
8.54IS
7.181CS,Od
14.06CS
13.13IS
12.58IS
10.35IS
8.875IS
7.124CS,0d
35.67ISII
24.01IS
14.62CS
13.59IS
12.58IS
11.38ISII
10.52IS
7.194CS,0d
2θ degrees

**Fig. 7**

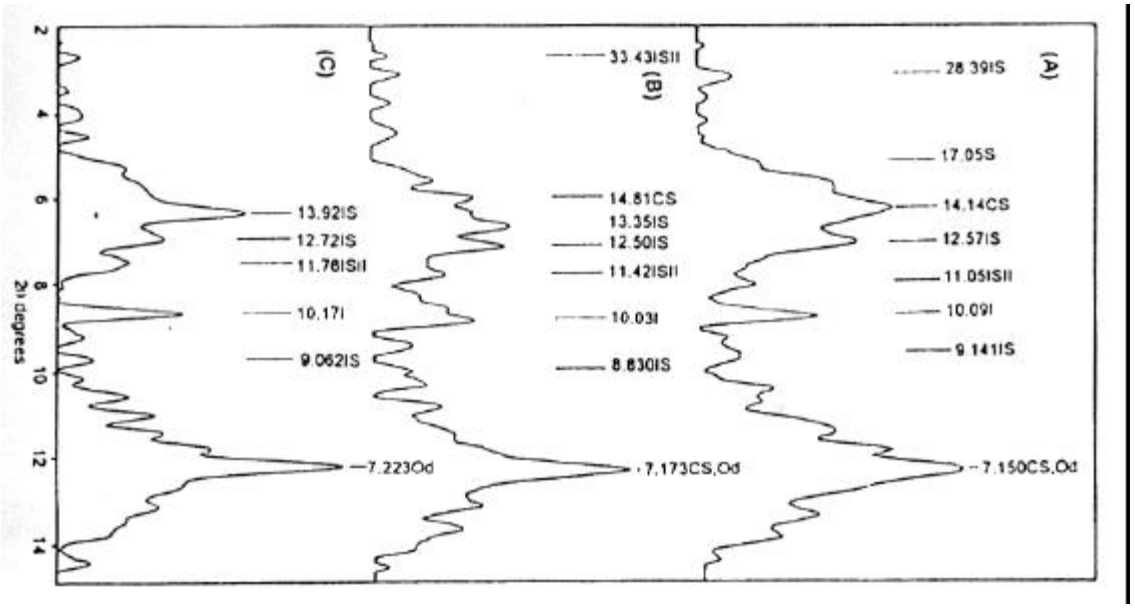
(C)
(B)
(A)
13.92IS
12.72IS
11.76ISII
10.17I
9.062IS
7.223Od
33.43ISII
14.81CS
13.35IS
12.50IS
11.42ISII
10.03I
8.830IS
7.173CS,Od
28.39IS
17.05S
14.14CS
12.57IS
11.05ISII
10.09I
9.141IS
7.150CS,Od
2θ degrees

**Fig. 8**

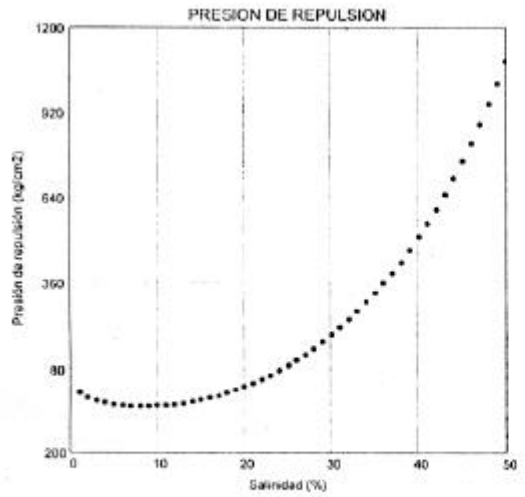


Figura 7B. Presión de repulsión, salmuera cálcica

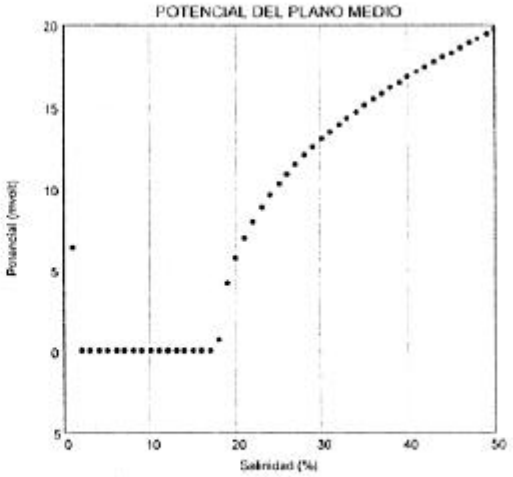


Figura 8B. Potencial del plano medio, salmuera cálcica

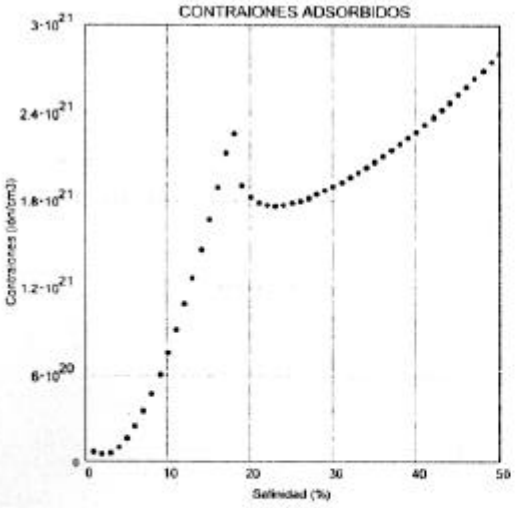


Figura 10B. Concentración de contraiones positivos adsorbidos, salmuera cálcica

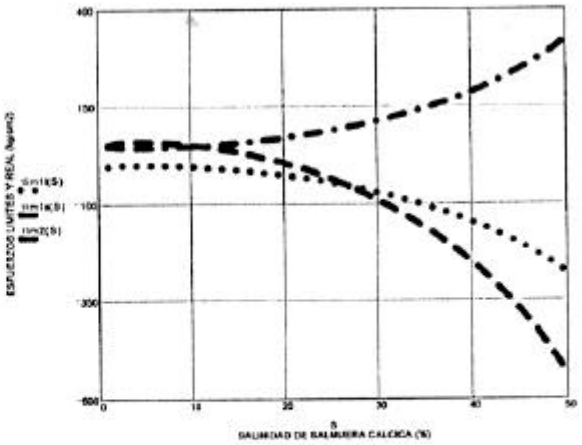


VARIACION DE LOS ESFUERZOS LIMITES Y REAL (CRITERIO DE FALLA MOHR-COULOMB) CON LA SALINIDAD DE LA SALMUERA CALCICA. LOS LIMITES DE SALINIDAD OCURREN A SALi = 10.843 Y SALs = 26.94

**Fig. 9**